FAST INTENT CLASSIFICATION FOR LLM ROUTING VIA STATISTICAL ANALYSIS OF REPRESENTATIONS

Anonymous authors
Paper under double-blind review

ABSTRACT

Intent classification in Large Language Models (LLMs) involves categorizing user prompts into predefined classes. For instance, given a user prompt, the system must determine whether it primarily concerns mathematics, coding, or general text processing. Such classification enables routing prompts to specialized models optimized for specific domains, improving both accuracy and computational efficiency. In this work, we introduce two lightweight, training-free methods based on statistical analysis of internal model representations and systematically compare them against baseline training-based approaches from the literature. Our methods analyze the distribution of key statistical metrics extracted from hidden features, enabling intent inference during the initial forward pass with minimal computational overhead. Through comprehensive empirical evaluation, we demonstrate that our training-free methods successfully classify prompts across varying levels of granularity—from high level distinctions (mathematics vs. coding vs. natural language) to fine-grained ones (e.g. Java vs. Python, etc). Our results provide a systematic characterization of scenarios where training-free methods are most useful, and identify cases where training-based approaches remain necessary, offering a practical guidance for deployment in production LLM systems.

1 INTRODUCTION

Large Language Models (LLMs) have demonstrated remarkable capabilities across diverse tasks including mathematical reasoning (Wei et al., 2022; Yao et al., 2023; Gao et al., 2023) and code generation (Li et al., 2022; Guo et al., 2024; Zhu et al., 2024). While many LLMs are trained for general purpose tasks (Radford et al., 2019; Raffel et al., 2020), current state-of-the-art is moving towards a routing approach where an intent classifier is used to detect user intent and then send the prompt to a specific model (OpenAI, 2025; Bocklisch et al., 2017; Bunk et al., 2020; Arora et al., 2024). This has the benefit of improving inference efficiency of production-scale LLM systems. Approaches to intent classification either rely on LLM calls, which is prone to hallucination (Bang et al., 2023; Banerjee et al., 2025), or on dedicated classification models, which requires extensive training data and computational resources Larson et al. (2019); Chen et al. (2019). Both introduce considerable inference latency and lack robust uncertainty quantification for routing decisions.

In this work, we introduce two training-free methods for intent classification, VecStat and NormStat, that operate entirely in the prefill phase with negligible extra cost. The motivation is the observation that different prompt types (mathematics, coding, general text, etc.) induce distinct activation distributions. Specifically, VecStat and NormStat represent two levels of statistical compression: VecStat preserves directional information but induces higher storage and calibration cost, while NormStat aggregates radial evidence and enjoys minimal memory consumption. Theoretical analysis further clarifies this trade-off: VecStat is preferable when class differences are primarily directional, whereas NormStat suffices—and is more memory-efficient—for isotropic-scale separation (coarse-grained classification tasks) thanks to the dimension-free calibration complexity.

Beyond computational efficiency relative to direct LLM calls, a key benefit of statistical methods is uncertainty quantification. With a one-line softmax normalization, statistical methods yield well-calibrated class probabilities, including on mixed-intent prompts; In contrast, we show that a training-based method using MLP head (inspired from sentence-classification pipelines (Casanueva et al., 2020; Jiang et al., 2024)) typically requires post-hoc calibration (e.g., temperature scaling)

Method	FLOPs Overhead	Memory Overhead	Extendability of New Classes	Uncertainty Quantification
NormStat	$O(Td)$	$O(m)$	Compute new baselines	Works well
VecStat	$O(Td)$	$O(md)$	Compute new baselines	Works well
MLP	$O(hd)$	$O(hd)$	Retrain a new MLP head	Possible but needs extra calibration
LLM Call	$\Omega(Td^2)$	$\sim$	Extend via prompt engineering	$\times$

Table 1: Comparison of classifiers. T: prompt length; d: hidden width; m: # classes; h: MLP hidden size.

to avoid overconfidence (Guo et al., 2017). When classes change, our methods also support rapid, incremental updates by simply appending new class statistics, avoiding any retraining. Table 1 compares these methods by compute, memory, extendability, and uncertainty quantification.

We conduct extensive empirical analysis to compare the performance of VecStat and NormStat against the training-based MLP classifier applied at the LLM's final projection layer. We apply these methods to LLMs ranging from 1B to 32B parameters and evaluate intent classification at both coarse-grained and fine-grained levels across seven benchmark datasets. The empirical results reveal that there is no one-fits-all model for intent classification. On the one hand, NormStat excels at coarse-grained intent classification with minimal computational and storage overhead, while VecStat handles both coarse-grained and fine-grained tasks but requires additional storage overhead. On the other hand, training-based methods typically achieve higher accuracy on hard tasks, yet they suffer from overconfidence in predictions, limiting their ability to provide reliable uncertainty quantification and making them vulnerable to ambiguous prompts. Our contributions are:

- We introduce NormStat and VecStat, two training-free statistical methods that perform intent classification directly within the LLM prefill phase, requiring $O(Td)$ additional computation compared to $\Theta(Td^2)$ forward pass cost, enabling deployment with negligible latency overhead.
- We provide theoretical analysis showing when each method excels: VecStat performs best when prompt types differ in feature directions, while NormStat is optimal when they differ in overall magnitude, with NormStat requiring fewer calibration samples to achieve comparable accuracy.
- We validate our methods across seven LLMs (1B-32B parameters) on both coarse-grained and fine-grained intent classification tasks, demonstrating that statistical methods provide superior uncertainty quantification for mixed-intent prompts compared to overconfident training-based approaches, while achieving competitive accuracy with minimal computational overhead. Furthermore, we show that statistics from early layers—available during the early prefill stage—are sufficient for accurate routing without a full forward pass, reducing serving-time computation.

1.1 Related Work

Task Classification Intent classification maps a user prompt to a predefined label. Classical approaches either (i) train supervised classifiers over tokenized utterances (e.g., CNNs) to produce a distribution over intents (Hashemi et al., 2016; Goo et al., 2018; He et al., 2019), or (ii) fine-tune contextual encoders, particularly BERT-based models, where hidden states feed specialized intent classification heads, often jointly trained with slot filling tasks (Chen et al., 2019; Bocklisch et al., 2017; Bunk et al., 2020). In modern LLM-based systems, intent classification serves as a critical routing mechanism that allows the selection of appropriate downstream tools and models, enforces guardrails and fallback policies, and optimizes inference cost and latency (Souha et al., 2023; Arora et al., 2024). The predominant approach involves direct LLM inference through several key techniques (Liu et al., 2023; Rodriguez et al., 2024; Wang et al., 2023; Arora et al., 2024; Hong et al., 2024; Wei et al., 2022). However, the computational expense of LLM inference at scale has motivated hybrid architectures that combine fast, lightweight classifiers (including PEFT-tuned encoders) with LLMs through uncertainty-aware routing mechanisms. These systems employ confidence thresholding, entropy-based measures, or learned routing policies to reserve expensive LLM calls for ambiguous cases where simpler models exhibit high uncertainty (Liu et al., 2022; 2024).

LLMs as text encoder Recent advances in LLMs have prompted researchers to explore their use as text encoders. An interesting approach is embedding extraction where existing methods typically operate on the last layer outputs through three strategies: using the last token embedding (Ma et al., 2024; Neelakantan et al., 2022; Wang et al., 2024; Meng et al., 2024; Jiang et al., 2024), averaging across all token embeddings (Muennighoff, 2022; Muennighoff et al., 2024; BehnamGhader et al.,

2024), or employing trainable modules (Lee et al., 2024; Tang & Yang, 2024). Interested readers can refer to (Tao et al., 2024; Nie et al., 2024) for a more detailed review on this topic. In contrast to these approaches, this work addresses user-intent classification for routing where both accuracy and computational efficiency are primary considerations. Our method utilizes prefill-time outputs from general-purpose LLMs without modification or additional training. By leveraging computational intermediates already produced during LLM prefill phase, this approach avoids the storage overhead of maintaining a dedicated billion-parameter model for intent classification.

Neural Feature Analysis Our approach extracts representations Wz, where W is a pretrained weight matrix and z is model's hidden state. This design is motivated by two lines of research. First, linear probes effectively extract semantic information from transformer representations (Alain & Bengio, 2016; Hewitt & Manning, 2019), with sparse autoencoder studies suggesting that many concepts are captured by a small number of sparse features in the activation space (Cunningham et al., 2024; Gao et al., 2024). Superposition theory provides theoretical grounding, explaining how features remain recoverable through linear projections (Elhage et al., 2022). Second, activation steering research demonstrates that intent-related behaviors can be manipulated through linear interventions in the representation space (Turner et al., 2023; Panickssery et al., 2023). Finally, activations Wz were successfully used in Hayou et al. (2025) to determine target module for LoRA finetuning, showing that activation capture data signal.

2 METHODOLOGY

In Large Language Models, prefill refers to the first forward pass of the user prompt. During this time, KV-cache is filled for autoregressive decoding (Shazeer, 2019; Ainslie et al., 2023; Chang et al., 2024; Aguirre et al., 2025; Jie et al., 2025) and gets updated for each token generation. In the prefill, we already compute the prompt's first forward pass to build keys/values; adding a light classifier there adds low cost but could provide a strong signal to route the prompt if needed: simple prompts remains on a small, cheap model; math/code/reasoning prompts routed to a larger or specialized model. Making this decision before the first generated token avoids wasting computation on the mismatched model. This is even more important if routing is customized for each user.

Modern LLM serving imposes a *lightweight* constraint on any prefill-time intent classifier used for routing: (i) the classifier's extra computation must be negligible compared to a single forward pass, and (ii) per-prompt memory and persistent storage must be negligible. Concretely, for a prompt of length T, a forward pass cost $\Theta(Td^2)$[1] computation in any given layer with hidden dimension d; a *lightweight* classifier should at most add $o(Td^2)$ cost, ideally $O(Td)$. Likewise, per-request state must be $O(1)$–$O(d)$ floats (not $O(Td)$), and per-class baselines must be $O(1)$–$O(d)$ numbers. More details are provided later in the paper.

In the following, we introduce a training-free approach to intent classification, based on a statistical analysis of hidden features in LLMs, and satisfies the computational constraints above.

2.1 A STATISTICAL APPROACH TO INTENT CLASSIFICATION

Consider an LLM with weight modules $\mathcal{M} = \{W_1, W_2, \ldots, W_p\}$, for some $p \geq 1$. The weights modules $\mathcal{M}$ represent all available weight matrices in the model, across layer index and module type. We will abuse the notation and use W_ℓ to refer to both the module and its weight matrix.

Let $\mathbf{x} = (x_t)_{1 \leq t \leq T}$ be a prompt of T tokens. For each weight module W_k, let $(y_{\ell,t})_{1 \leq t \leq T}$ denote the output features in module W_ℓ. For instance, $(y_{\ell,t})_{1 \leq t \leq T}$ could be the output of a Query head, or the projection layer in an MLP block. Each $y_{\ell,t}$ is a d-dimensional vector given by $y_{\ell,t} = W_\ell z_{\ell,t}$, where d is the output dimension in module W_ℓ, and $z_{\ell,t}$ is the input to that module for token t.

Intent classification. We aim to classify the prompt $\mathbf{x}$ into one of the classes $C_1, C_2, \ldots, C_m$, where $m \geq 2$. For instance, a binary classification where C_1 is mathematics and C_2 is coding. For

[1]The forward pass cost is $\Theta(Td^2 + T^2d)$. In the regime $d > T$, the Td^2 term dominates, so we drop the T^2d term and write the cost as $\Theta(Td^2)$; retaining T^2d does not affect our conclusions.

each module W_ℓ, we compute lightweight summary statistics from the features $\{y_{\ell,t}\}_{t=1}^T$ and compare them to per-class baselines: (i) for each class C_i, precompute the same statistics on *calibration data* at the same module W_ℓ; (ii) for the incoming prompt, compute the statistics at W_ℓ and measure similarity to each baseline; (iii) predict the class C_i with the highest similarity.

Several statistics are considered, such as the mean and covariance of $\{y_{\ell,t}\}_{t=1}^T$, to capture geometric information about the hidden features. Estimating the mean requires $O(Td)$ calculations while the covariance requires $O(Td^2)$. Therefore, using covariance is not computationally efficient in inference setting, since it violates the $O(Td)$ condition above. However, we consider a weaker variant where we only estimate coordinate-wise variance (diagonal of the covariance matrix). We call this method VecStat, which relies on coordinate-wise mean and variance for classification. We also introduce a lighter weight method called NormStat, which relies solely on the norm statistic across all tokens and coordinates.

In the following, we present the two methods in the single-layer case. When multiple layers are used, we aggregate similarity scores across ℓ by averaging.

Vector Statistic (VecStat): calculate *coordinate-wise* token means and second moments tokens

$$S_{\text{vec}} = \frac{1}{T}\sum_{t=1}^{T} y_t \in \mathbb{R}^d, \qquad Q_{\text{vec}} = \frac{1}{T-1}\sum_{t=1}^{T}(y_t - S_{\text{vec}}) \odot (y_t - S_{\text{vec}}) \in \mathbb{R}^d. \tag{1}$$

Norm Statistic (NormStat): summarize each y_t through a the norm $\|y_t\|$ and aggregate across tokens to obtain the statistics

$$S_{\text{norm}} = \frac{1}{T}\sum_{t=1}^{T} \frac{\|y_t\|}{\sqrt{d}} \in \mathbb{R}, \quad Q_{\text{norm}} = \frac{1}{T-1}\sum_{t=1}^{T}\left(\frac{\|y_t\|}{\sqrt{d}} - S_{\text{norm}}\right)^2 \in \mathbb{R}. \tag{2}$$

With both methods, we use closed-form Gaussian KL divergence (5) and (6) to measure the similarity between prompt and classes' statistics. Intuitively, this acts as a proxy for the true KL-divergence between distributions which is prohibitively expensive to compute. Across models and datasets, we observed that the radial token features $\|y_{\ell,t}\|/\sqrt{d}$ are Gaussian-like for fixed ℓ (Fig. 1), and similar observations hold for the coordinates of y_t. [2]

These two choices form a *statistical compression ladder*: VecStat keeps per-coordinate first and second moments, while NormStat compresses all coordinates to a single *radial* information per token and then to its mean/variance across tokens.

The rest of this section develops this story rigorously: (i) we prove when each is statistically preferable using a simplified Gaussian setting, and (ii) we connect those guarantees to *compute*, *memory*, and *calibration* costs. All the proofs are deferred to Appendix B.

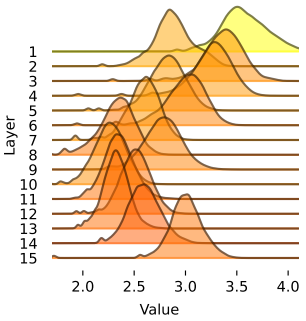

Figure 1: **Per-token query-norm distributions across layers.** Histograms of $\{\|y_{\ell,t}\|/\sqrt{d}\}_{t=1}^T$ for representative layers ℓ. Shapes are close to Gaussian with layer-dependent mean/variance, which supports a 1D Gaussian proxy for NormStat.

2.2 Intuitive Analysis in a Gaussian Setting

Intuitively, VecStat retains more information about feature distribution than NormStat because it tracks coordinate-wise statistics instead of a single statistic for each module. To understand the difference between these two methods, we consider a Gaussian setting with diagonal covariance and study regimes where NormStat is competitive with VecStat, in which case NormStat is preferred for computational efficiency. Additional analysis is in Appendix A.

Setting and notation. Here we study general features $(y_t)_{1\le t\le T}$ (not necessarily representations in an LLM). For each baseline class $k \in \{1,\dots,m\}$ and tokens $t = 1,\dots,T$, assume that

$$y_t \mid k \sim \mathcal{N}(\mu_k,\ \Sigma_k) \subset \mathbb{R}^d, \qquad \text{independently across } t, \tag{3}$$

[2] One could estimate an empirical KL without summaries, but doing so robustly at inference time is prohibitively expensive in both compute and memory.

where, $\Sigma_k = \mathrm{Diag}(\sigma_{k,1}^2, \ldots, \sigma_{k,d}^2)$ is a diagonal covariance matrix.

NormStat observes only the norm $\{\|y_t\|\}$ and is invariant to rotations of the features; it cannot detect separation that lives in direction. In contrast, VecStat retains per-coordinate first/second moments and is therefore rotation-sensitive. In an *isotropic-scale* setting (equal means, spherical covariances with different variance), the optimal likelihood ratio reduces to a monotone function of the total radial sum $\sum_t \|y_t\|^2$, so NormStat is already Bayes-optimal. But in a *directional* setting (equal covariance, equal mean norms, different mean directions), every radius-only rule is blind, whereas a coordinate-aware test achieves exponentially small error in T. The next theorem formalizes this.

Theorem 1. *[NormStat vs VecStat] Assume a binary classification $k \in \{1, 2\}$ with uniform prior.*

1. ***Directional regime (NormStat×, VecStat✓).*** *Assume $\Sigma_1 = \Sigma_2 = \sigma^2 I_d$, $\|\mu_1\| = \|\mu_2\|$, and $\mu_1 \neq \mu_2$. Then any classifier whose decision depends only on the norms $\{\|y_t\|\}_{t=1}^T$ has Bayes error $1/2$. Moreover, the likelihood-ratio test achieves error probability*
$$\Pr(\hat{k} \neq k) \leq \exp\left(-\frac{T}{8\sigma^2}\|\mu_1 - \mu_2\|^2\right), \quad \textit{where } \hat{k}(y_{1:T}) := \begin{cases} 1, & \langle S_{\mathrm{vec}}, \mu_1 - \mu_2 \rangle \geq 0, \\ 2, & \textit{otherwise.} \end{cases}$$

2. ***Isotropic-scale regime (NormStat✓, VecStat ties).*** *Assume $\mu_1 = \mu_2 = 0$ and $\Sigma_k = \sigma_k^2 I_d$ with $\sigma_1 \neq \sigma_2$. Then the Log-Likelihood Ratio is a strictly monotone function of the radial statistic $R_T := \sum_{t=1}^T \|y_t\|^2$; hence every Bayes-optimal test depends only on R_T, and adding coordinate-wise information cannot improve its Bayes risk.*

Theorem 1 isolates two extremes, whereas real prompts generally result in a mix between these extremes. An example is the following: assume y_t are i.i.d. from a sign–mixture with $s_t \in \{\pm 1\}$,

$$y_t \sim \pi\mathcal{N}(+\mu, \sigma^2 I_d) + (1-\pi)\mathcal{N}(-\mu, \sigma^2 I_d), \quad \gamma := \mathbb{E}[s_t] = 2\pi - 1,$$

where $\mu \in \mathbb{R}^d$, $\pi \in (0, 1)$. Hence,

$$\mathbb{E}[S_{\mathrm{vec}}] = \gamma\mu, \qquad \mathbb{E}[Q_{\mathrm{vec}}] = \sigma^2 \mathbf{1}_d + (1-\gamma^2)\,\mu \odot \mu, \qquad \mathbb{E}[S_{norm}] = \mathbb{E}\|y_t\| = F(\mu, \sigma^2),$$

where $F(\mu, \sigma^2)$ depends only on (μ, σ^2). For NormStat, since norms are even, the distribution of $\|y_t\|$ is invariant under the $\pm\mu$ mixture. Consequently, the distributions of S_{norm} and Q_{norm} do not depend on π. As $\pi \to \frac{1}{2}$, the advantage of VecStat over NormStat shrinks; at $\pi = \frac{1}{2}$, the mean component S_{vec} cancels, and VecStat effectively reduces to its second–moment part, aligning with the radial evidence summarized by NormStat. Away from $\frac{1}{2}$, S_{vec} provides a clear benefit.

Calibration Cost. An important aspect of statistical methods is sample complexity, or more specifically, the convergence rate in the number of samples. This provides an estimate of the total number of calibration samples needed to create the classes $k \in \{1, 2, \ldots, m\}$. The next theorem show the calibration advantage of NormStat over VecStat.

Theorem 2 (Calibration cost)**.** *Fix a class k. Let $y_1, \ldots, y_N \overset{i.i.d.}{\sim} \mathcal{N}(\mu_k, \Sigma_k)$ in $\mathbb{R}^d$, where N is the number of calibration samples drawn for this class. Let $q = \mathbb{E}[\|y_1\|]$ and define $\hat{\mu}_k = N^{-1}\sum_{i=1}^N y_i$, and $\hat{q} = N^{-1}\sum_{i=1}^N d^{-1/2}\|y_i\|$. Then, for any $\delta \in (0, 1)$, with probability at least $1 - \delta$, we have:*

1. ***NormStat (dimension-free):*** $|\hat{q} - q| \lesssim \sqrt{\frac{\log(1/\delta)}{N}}$.

2. ***VecStat (dimension-dependent):*** $\|\hat{\mu}_k - \mu_k\|_2 \lesssim \sqrt{\frac{d + \log(1/\delta)}{N}}$.

Considering just the statistics $\hat{\mu}$ and $\hat{q}$, to obtain an estimation error of order ϵ, one needs $N = \Omega(\epsilon^{-2})$ for $\hat{q}$ and $N = \Omega(d\epsilon^{-2})$ for $\hat{\mu}$, showing the computational advantage of NormStat over VecStat. This is particularly important in data scarce regimes with few samples for each class. We discuss this in more details in the next section.

Theorem 1 and Theorem 2 compare our methods from two different angles: (i) expressivity, where VecStat has an edge if directional information is important, otherwise NormStatties with VecStat, (ii) calibration cost, where NormStat has an edge with fewer calibration samples needed to reach a given error level. A third important angle is storage/memory cost: while both methods have similar classification cost ($O(Td)$ per module), NormStat uses $O(B)$ scalars and $O(B)$ scoring FLOPs, while VecStat uses $O(Bd)$ numbers and $O(Bd)$ scoring FLOPs—so for large B or tight memory/latency budgets, NormStat has an advantage.

2.3 TRAINING-BASED INTENT CLASSIFICATION

For a comprehensive empirical study, we consider an intent classifier based on a trained head on top of frozen LLM features. We use the last Transformer block and write $y_{\ell^\star,t} \in \mathbb{R}^d$ for its token features ($t = 1, \ldots, T$). Inspired by prompt/sentence classification pipelines (e.g., (Ma et al., 2024; Wang et al., 2024; Meng et al., 2024)), we build a single prompt-level vector in two ways:

$$\textbf{Avg-MLP:} \quad z_{\text{avg}} := \frac{1}{T}\sum_{t=1}^{T} y_{\ell^\star,t} = S_{\text{vec}}^{(\ell^\star)} \in \mathbb{R}^d, \qquad \textbf{Tail-MLP:} \quad z_{\text{tail}} := y_{\ell^\star,T} \in \mathbb{R}^d.$$

Given $z \in \{z_{\text{avg}}, z_{\text{tail}}\}$, we train a two-layer MLP with hidden width h with cross entropy loss. Since z_{avg} or z_{tail} is produced during prefill, the incremental latency is a single MLP forward pass.

Compute/memory and deployment. Per token, the head adds $O(dh + hm)$ FLOPs and stores $O(dh + hm)$ parameters, with $m \ll d$ in our setting. Post-hoc calibration (e.g., temperature scaling on a held-out split) yields better-calibrated confidences for routing. Because the head is small, per-user heads are feasible; however, unlike NormStat/VecStat, adding a new baseline class expands the output layer and typically requires retraining or incremental fine-tuning. Empirically, Avg-MLP is more stable for long prompts, while Tail-MLP can capture end-of-prompt cues.

3 EXPERIMENTS

In this section, we evaluate the effectiveness of NormStat, VecStat, Avg-MLP and Tail-MLP across multiple LLMs and classification datasets.[3] Comprehensive experimental details can be found in Appendix C, and additional experimental results are presented in Appendix D.

3.1 EXPERIMENTAL SETUP

Classification granularities We consider two levels of granularity. Level-1 addresses coarse-grained classification across three domains: general text, mathematics, and code. Level-2 tests fine-grained separation within each domain: identifying programming languages, mathematical subfields, natural languages. For Level-1 calibration, we use representative datasets: MMLU European History (Hendrycks et al., 2021a;b) for general text, GSM8K (Cobbe et al., 2021) for mathematics, and Magicoder (Wei et al., 2023) for code. We test on MMLU US History for general text, GSM8K and MATH500 (Lightman et al., 2023) for mathematics (in-distribution and out-of-distribution respectively), and Magicoder and HumanEval (Chen et al., 2021) for code (in/out of distribution). Level-2 experiments utilize domain-specific subsets: Magicoder for programming language identification, Competition Math (Hendrycks et al., 2021c) for mathematical subfield classification, and the Aya dataset (Singh et al., 2024) for natural language identification, with each dataset split between calibration and test sets. For more details, please refer to Appendix C.1.

Method and LLM selection We compare five classification methods: our methods NormStat and VecStat, with VecStat evaluated using both cosine similarity (VecStat:Cos) and KL divergence (VecStat:KL), and training-based baselines Avg-MLP) and (Tail-MLP). Training-based methods use the same calibration data for training to ensure fair comparison. All calibration prompts are truncated to 512 tokens, with training-free methods probing all projection modules across LLMs. We evaluate on seven pretrained LLMs from the Qwen3 and Llama families, spanning 1B to 32B parameters and including both base and instruction-tuned variants, providing comprehensive coverage across model scales and training paradigms. See Appendix C.3 for more details on the selected LLMs.

Evaluation Metrics We compute accuracy on each test dataset independently, where each dataset contains samples from a single ground-truth class. This approach ensures our evaluation is not biased by varying dataset sizes across classes. For Level-2 classification, we report mean accuracy across all classes within each task due to space constraints. This mean accuracy corresponds to the balanced accuracy metric, providing equal weight to each class regardless of test set size and effectively handling the natural class imbalance among test datasets. All experiments use three random seeds, and we report mean performance with standard deviation.

[3] Source code is provided in the supplemental materials

Table 2: Classification accuracy across five methods on level-1 and level-2 classification granularities. Level-1 reports per-dataset accuracy for coarse-grained domain classification (general text, math, code). Level-2 reports average accuracy across classes within each domain: programming languages, mathematical subfields, and natural languages. Qwen3-32B natural language results are omitted due to computational constraints.

Model	Method	Level-1					Level-2		
		gsm8k	humaneval	magicoder	math500	mmlu_history	code	math	natural language
Qwen3-1.7B	Avg-MLP	99.97±0.04	99.80±0.35	99.99±0.02	78.33±1.67	100.00±0.00	99.96±0.01	76.77±0.27	99.93±0.02
	Tail-MLP	100.00±0.00	100.00±0.00	99.97±0.02	99.00±0.00	100.00±0.00	99.59±0.02	72.12±0.27	99.87±0.05
	NormStat:KL	97.35±0.00	70.12±0.61	99.27±0.11	76.60±0.20	100.00±0.00	57.79±0.73	38.39±0.56	89.77±0.25
	VecStat:KL	100.00±0.00	99.39±0.00	99.97±0.03	88.33±0.30	100.00±0.00	99.24±0.12	48.36±0.64	99.20±0.08
	VecStat:Cos	100.00±0.00	98.78±0.00	99.97±0.03	92.26±0.11	100.00±0.00	99.08±0.16	52.74±0.67	99.57±0.02
Llama-3.2-1B	Avg-MLP	100.00±0.00	100.00±0.00	99.99±0.01	64.33±8.33	99.84±0.28	99.97±0.01	70.20±0.72	99.91±0.04
	Tail-MLP	99.95±0.04	100.00±0.00	99.97±0.03	98.93±0.42	99.35±1.13	99.47±0.07	69.01±1.11	99.83±0.07
	NormStat:KL	99.49±0.09	90.85±0.00	96.39±0.20	83.40±0.00	92.48±0.57	49.22±0.73	31.27±0.54	86.53±1.33
	VecStat:KL	100.00±0.00	99.39±0.00	99.98±0.02	78.80±0.12	100.00±0.00	98.99±0.10	47.67±0.89	99.19±0.08
	VecStat:Cos	100.00±0.00	99.39±0.00	99.97±0.02	77.60±0.20	100.00±0.00	98.71±0.12	51.47±0.73	99.72±0.01
Qwen3-8B	Avg-MLP	99.42±0.74	99.59±0.35	99.99±0.02	77.27±11.02	100.00±0.00	99.97±0.01	79.10±0.48	99.92±0.01
	Tail-MLP	99.82±0.12	98.58±2.46	99.98±0.02	81.20±9.72	100.00±0.00	99.67±0.01	75.76±0.68	99.88±0.04
	NormStat:KL	85.14±0.35	10.37±1.06	99.85±0.06	92.93±0.12	99.51±0.49	56.39±0.69	33.25±0.92	90.09±0.40
	VecStat:KL	99.95±0.04	99.59±0.35	99.99±0.02	92.20±0.00	100.00±0.00	99.23±0.10	49.99±1.12	99.20±0.08
	VecStat:Cos	100.00±0.00	95.73±0.61	99.98±0.03	94.20±0.00	100.00±0.00	99.34±0.09	54.75±0.63	99.68±0.03
Qwen3-32B	Avg-MLP	95.88±3.31	100.00±0.00	99.99±0.01	86.87±5.22	100.00±0.00	99.97±0.01	78.67±0.67	
	Tail-MLP	99.39±0.00	100.00±0.00	99.98±0.00	96.80±0.40	99.02±0.49	98.41±0.10	74.07±1.15	
	NormStat:KL	97.93±0.04	24.59±0.35	99.78±0.06	97.93±0.12	100.00±0.00	57.03±0.43	35.14±0.25	-
	VecStat:KL	100.00±0.00	99.39±0.00	99.98±0.03	96.60±0.00	100.00±0.00	99.53±0.07	53.16±0.52	
	VecStat:Cos	100.00±0.00	98.17±0.00	99.98±0.03	96.80±0.35	100.00±0.00	99.61±0.06	56.70±0.88	

3.2 Empirical Results

Table 2 reports classification results at both granularity levels for five methods on four representative LLMs, while Table 3 provides detailed per-class accuracy for level-2 programming language classification. Results for all seven LLMs are reported in Appendix D.1 (level-1) and D.2 (level-2).

Level-1 classification performance Across coarse-grained intent classification, all methods achieve strong performance on in-distribution test sets. The effectiveness of NormStat, despite using only radial statistics, demonstrates itself as a computational- and memory-efficient approach when the classes are different enough. Surprisingly, NormStat outperforms all other methods in some cases (e.g. Qwen3-32B evaluated on math500). VecStat achieves marginally higher accuracies than NormStat in most cases, however, this improvement comes at increased computational cost. Training-based methods perform comparably to VecStat, with no approach consistently dominating across datasets. Out-of-distribution generalization varies substantially, as evidenced by the performance difference between GSM8K and MATH500 for mathematics tasks, suggesting that different methods might capture distinct aspects of domain characteristics.

Level-2 classification performance Fine-grained classification within domains reveals clear performance stratification across methods. For programming language identification, VecStat maintains near-perfect accuracy while NormStat shows substantial degradation, aligning with our theoretical prediction that directional information becomes critical for within-domain discrimination. As detailed in Table 3, this performance gap remains consistent across all nine programming languages. Mathematical subfield classification proves most challenging for training-free methods, with both NormStat and VecStat falling short of training-based approaches. This gap suggests that effective discrimination among mathematical topics requires non-linear transformations better captured through supervised training signals. In contrast, natural language identification demonstrates strong performance across all methods, with VecStat achieving near-perfect accuracy, likely due to distinct linguistic features being well-separated in the LLM's hidden representation space.

Distance metric comparison The cosine distance variant of VecStat consistently outperforms its KL divergence counterpart, particularly in Level-2 tasks. This may suggest that the independence assumption across feature dimensions inherent in the diagonal covariance formulation may discard correlational information present in the true feature distributions. On the contrary, angular separation between prompt and baseline statistics offers a more robust measure that captures directionality.

Table 3: Level-2 programming language classification results for Qwen3-8B and Qwen3-32B. Values represent per-class accuracy across nine programming languages from the Magicoder.

Model	Method	cpp	csharp	java	php	python	rust	shell	swift	typescript
Qwen3-8B	Avg-MLP	99.95±0.05	100.00±0.00	100.00±0.00	99.96±0.06	99.91±0.01	100.00±0.00	100.00±0.00	100.00±0.00	99.94±0.03
	Tail-MLP	99.61±0.16	99.69±0.18	99.47±0.12	100.00±0.00	99.39±0.22	99.53±0.10	99.92±0.14	99.75±0.07	99.61±0.10
	NormStat:KL	47.37±0.94	38.26±1.28	27.59±0.65	60.14±1.27	67.73±0.54	63.05±0.43	91.51±0.60	62.54±1.25	49.28±0.84
	VecStat:KL	99.09±0.11	98.58±0.42	97.78±0.09	99.78±0.22	99.01±0.04	99.81±0.00	99.76±0.00	99.91±0.09	99.38±0.20
	VecStat:Cos	98.90±0.24	98.96±0.38	98.49±0.03	99.85±0.13	99.13±0.12	99.55±0.07	100.00±0.00	99.81±0.12	99.35±0.19
Qwen3-32B	Avg-MLP	99.91±0.03	99.98±0.04	100.00±0.00	99.96±0.06	99.91±0.03	99.97±0.06	100.00±0.00	100.00±0.00	99.96±0.04
	Tail-MLP	98.01±0.41	97.27±0.95	97.99±0.53	98.77±0.22	98.26±0.21	99.21±0.06	98.97±0.60	98.71±0.48	98.50±0.07
	NormStat:KL	53.57±0.94	36.94±1.38	25.47±1.43	59.47±0.57	61.66±1.40	67.63±0.54	89.29±0.71	69.35±1.19	49.84±1.08
	VecStat:KL	99.01±0.11	99.35±0.34	98.72±0.03	99.89±0.11	99.29±0.06	99.90±0.05	100.00±0.00	99.85±0.09	99.75±0.16
	VecStat:Cos	99.18±0.14	99.53±0.19	99.01±0.10	99.89±0.11	99.50±0.04	99.81±0.13	100.00±0.00	99.87±0.12	99.72±0.09

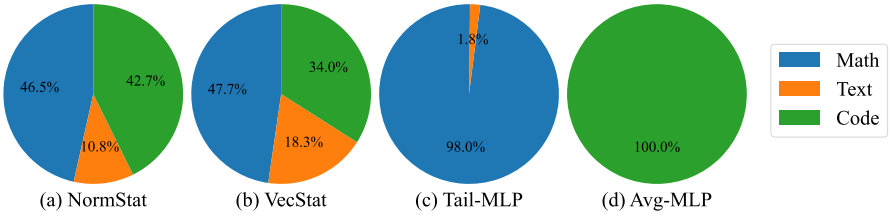

(a) NormStat (b) VecStat (c) Tail-MLP (d) Avg-MLP

Figure 2: Uncertainty quantification results on a mixed-intent prompt on Qwen-1.7B-Base.

3.3 Case study on ambiguous prompts

We examine classification uncertainty of different methods when encountering ambiguous prompts with mixed intents. We concatenate programming and mathematical content into a single prompt and analyze the resulting prediction distributions across all three level-1 categories. For NormStat and VecStat, we form probabilities via a softmax over negative distances $p_i \propto \exp\big(-d_i/\tau\big)$, and rescale distances with a problem-scale constant $\tau = O(\text{distance})$ before the softmax (in our experiments, $\tau = 10$). This temperature-like scaling yields meaningful confidence estimates with essentially zero extra cost. In contrast, the training-based approaches (Avg-MLP and Tail-MLP) take the softmax of MLP logits; these probabilities are not calibrated by default, and obtaining reliable uncertainty quantification requires an explicit post-hoc calibration step (e.g., temperature scaling learned on a validation set) (Guo et al., 2017), which we do not apply here.

Both VecStat and NormStat (Fig. 2(a)–(b)) produce well-calibrated distributions that reflect the prompt's mixed nature—assigning substantial mass to both math and code while down-weighting text. In contrast, the training-based methods (Fig. 2(c)–(d)) are overconfident, placing essentially all mass on a single class despite mixed content. This failure stems from discriminative training on clean data yielding overly sharp decision boundaries that are poorly calibrated for out-of-distribution, noisy inputs. While such predictions can score well on clean test sets, they produce misleading uncertainty in deployment scenarios where mixed-intent prompts naturally occur (see Appendix D.3).

3.4 Effect of number of probed layers and prompt length

Number of probed layers Fig. 3 visualizes the impact of number of probed layers (counted from the first layer) on level-1 accuracy. VecStat demonstrates a robust performance regardless of layer count, indicating that early layers capture sufficient statistical information for intent classification without requiring information from deeper layers. In contrast, NormStat exhibits dataset-dependent behavior: performance degrades with additional layers on humaneval but improves on math500, though both achieve competitive accuracy using only the first 12 layers out of 28. These findings have important practical implications for deployment efficiency. Since accurate classification is achievable using only the initial layers' statistics—computed during the early stages of prefill—routing can be performed without completing a full forward pass, substantially saving computation costs when prompts are redirected to different LLMs. See Appendix D.4 for additional results.

Maximum prompt length Fig. 4 examines the impact of sequence length on classification accuracy for Qwen3-1.7B. The results reveal distinct patterns in prompt length sensitivity across different statistical methods. VecStat demonstrates remarkable stability, maintaining near-optimal accuracy across all sequence lengths from 32 to 512 tokens for both datasets. This robustness indicates that

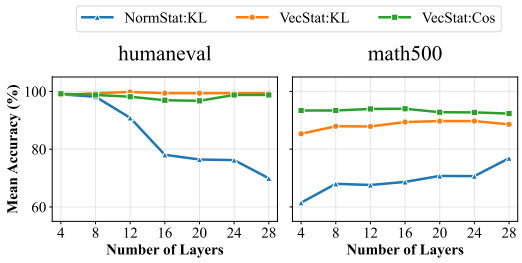

Figure 3: Effect of the number of layers on level-1 classification accuracy for Qwen3-1.7B.

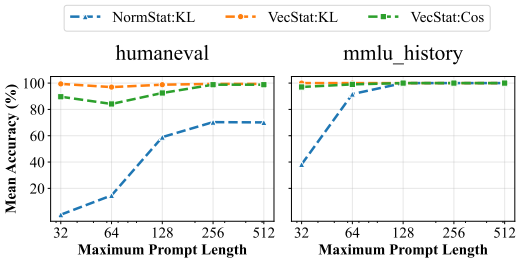

Figure 4: Effect of the maximum prompt length on level-1 classification for Qwen3-1.7B.

coordinate-wise statistics capture sufficient discriminative information even from truncated prompts, enabling potential deployment optimizations through reduced sequence lengths (64-128 tokens) that could significantly improve throughput without compromising intent classification performance. NormStat is more sensitive to prompt length, with accuracy improving substantially as length increases and plateauing at approximately 128 tokens. The strong correlation between prompt length and accuracy for radial statistics suggests that accumulating sufficient statistical evidence requires slightly longer contextual windows. More detailed results are presented in Appendix D.6.

3.5 Calibration Analysis

To validate Theorem 2, we compare the empirical and theoretical convergence rates of NormStat and VecStat on the MagiCoder dataset and present the result in Fig. 5. We vary the calibration sample size from 512 to 32768 and conduct multiple runs with different seeds. Our results demonstrate strong empirical match with the theoretical bounds. Both methods show $\tilde{O}(N^{-0.5})$ rate for the mean error, following the predicted theoretical curves. Notably, NormStat attains much lower absolute errors, which is consistent with its dimension-free bound, whereas VecStat sits higher due to its dimension-dependent bounds. Calibration results for other LLMs are deferred to Appendix D.5.

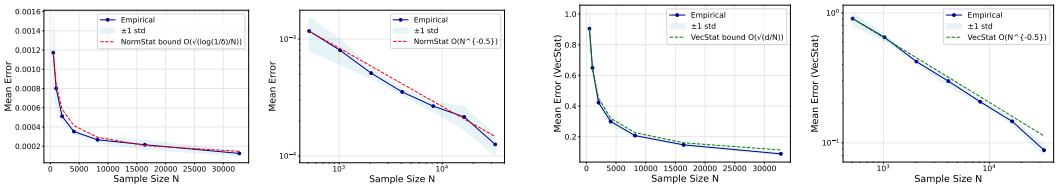

(a) NormStat (b) VecStat

Figure 5: Calibration convergence analysis for Qwen3-8B on the MagiCoder dataset. Each subplot shows both linear and log-log scales comparing empirical results with theoretical bounds.

4 Conclusion

We presented prefill-time, training-free intent classifiers—NormStat and VecStat—that provide fast, uncertainty-aware routing with $O(Td)$ FLOPs overhead, and compared them with two training-based methods (Avg-MLP, Tail-MLP). Our theory pinpoints when each statistic is preferable: VecStat is more accurate in directional regimes where class differences reside in feature orientation, while NormStat is Bayes-optimal in isotropic-scale regimes and enjoys dimension-free calibration cost. Empirically, across 1B–32B LLMs and both coarse- and fine-grained settings, VecStat attains near-perfect accuracy on fine-grained tasks, whereas NormStat delivers competitive coarse-grained accuracy with the smallest memory/latency footprint. Accurate uncertainty estimates can be obtained for both statistical methods at essentially no extra cost, in contrast to MLP heads that typically require post-hoc calibration. Practically, NormStat is most useful in low-latency settings with frequently updated routers; VecStat is useful when a more fine-grained routing is needed; and learned MLP head is useful for cases where marginal accuracy gains justify calibration and maintenance. Finally, we empirically show that early-layer statistics are informative, enabling early-exit routing that saves compute by deciding before a full pass completes.

STATEMENT OF AUTHORS

ETHICS STATEMENT

We adhere to the ICLR Code of Ethics. Our study does not involve human subjects, personally identifiable information, or sensitive attributes; all datasets are publicly available under permissive licenses, and we follow their terms of use. We neither collect new data nor perform any form of user profiling, re-identification, or demographic inference. We evaluate and report results using standard, publicly accepted protocols, and we avoid releasing models or artifacts that are reasonably likely to enable harmful applications. We disclose computing resources and consider environmental impact in our experiments; no conflicts of interest or external sponsorships influenced the work. The authors take full responsibility for the integrity and accuracy of the content.

REPRODUCIBILITY STATEMENT

We provide runnable code in the supplementary materials. The full codebase will be released as open-source after the review process. All experimental settings—including dataset specifications, preprocessing steps, training/evaluation pipelines, and exact hyperparameters—are documented in the appendix for complete reproducibility.

THE USE OF LARGE LANGUAGE MODELS

We used LLMs solely as general-purpose assistive tools. For writing, we employed OpenAI's GPT-5 to polish language in sentence level—improving clarity, grammar, and style—without generating scientific claims, interpreting results, or drafting sections de novo. For coding, we used the Cursor IDE's built-in autocomplete to suggest boilerplate and minor edits; all coding/writing logic was authored, reviewed, and verified by the authors. The research ideas, experimental design, and overall manuscript structure were conceived and developed by the authors without any LLM involvement. The authors take full responsibility for the content.

REFERENCES

Maia Aguirre, Ariane Méndez, Arantza Del Pozo, María Inés Torres, and Manuel Torralbo. Fine-tuning medium-scale llms for joint intent classification and slot filling: A data-efficient and cost-effective solution for smes. In *Proceedings of the 31st International Conference on Computational Linguistics: Industry Track*, pp. 251–262, 2025.

Joshua Ainslie, James Lee-Thorp, Michiel De Jong, Yury Zemlyanskiy, Federico Lebrón, and Sumit Sanghai. Gqa: Training generalized multi-query transformer models from multi-head checkpoints. *arXiv preprint arXiv:2305.13245*, 2023.

Guillaume Alain and Yoshua Bengio. Understanding intermediate layers using linear classifier probes. *arXiv preprint arXiv:1610.01644*, 2016.

Gaurav Arora, Shreya Jain, and Srujana Merugu. Intent detection in the age of llms. *arXiv preprint arXiv:2410.01627*, 2024.

Sourav Banerjee, Ayushi Agarwal, and Saloni Singla. Llms will always hallucinate, and we need to live with this. In *Intelligent Systems Conference*, pp. 624–648. Springer, 2025.

Yejin Bang, Samuel Cahyawijaya, Nayeon Lee, Wenliang Dai, Dan Su, Bryan Wilie, Holy Lovenia, Ziwei Ji, Tiezheng Yu, Willy Chung, et al. A multitask, multilingual, multimodal evaluation of chatgpt on reasoning, hallucination, and interactivity. *arXiv preprint arXiv:2302.04023*, 2023.

Parishad BehnamGhader, Vaibhav Adlakha, Marius Mosbach, Dzmitry Bahdanau, Nicolas Chapados, and Siva Reddy. Llm2vec: Large language models are secretly powerful text encoders. *arXiv preprint arXiv:2404.05961*, 2024.

Tom Bocklisch, Joey Faulkner, Nick Pawlowski, and Alan Nichol. Rasa: Open source language understanding and dialogue management. *arXiv preprint arXiv:1712.05181*, 2017.

Tanja Bunk, Daksh Varshneya, Vladimir Vlasov, and Alan Nichol. Diet: Lightweight language understanding for dialogue systems. *arXiv preprint arXiv:2004.09936*, 2020.

Iñigo Casanueva, Tadas Temčinas, Daniela Gerz, Matthew Henderson, and Ivan Vulić. Efficient intent detection with dual sentence encoders. *arXiv preprint arXiv:2003.04807*, 2020.

Chi-Chih Chang, Wei-Cheng Lin, Chien-Yu Lin, Chong-Yan Chen, Yu-Fang Hu, Pei-Shuo Wang, Ning-Chi Huang, Luis Ceze, Mohamed S Abdelfattah, and Kai-Chiang Wu. Palu: Compressing kv-cache with low-rank projection. *arXiv preprint arXiv:2407.21118*, 2024.

Mark Chen, Jerry Tworek, Heewoo Jun, Qiming Yuan, Henrique Ponde de Oliveira Pinto, Jared Kaplan, Harri Edwards, Yuri Burda, Nicholas Joseph, Greg Brockman, Alex Ray, Raul Puri, Gretchen Krueger, Michael Petrov, Heidy Khlaaf, Girish Sastry, Pamela Mishkin, Brooke Chan, Scott Gray, Nick Ryder, Mikhail Pavlov, Alethea Power, Lukasz Kaiser, Mohammad Bavarian, Clemens Winter, Philippe Tillet, Felipe Petroski Such, Dave Cummings, Matthias Plappert, Fotios Chantzis, Elizabeth Barnes, Ariel Herbert-Voss, William Hebgen Guss, Alex Nichol, Alex Paino, Nikolas Tezak, Jie Tang, Igor Babuschkin, Suchir Balaji, Shantanu Jain, William Saunders, Christopher Hesse, Andrew N. Carr, Jan Leike, Josh Achiam, Vedant Misra, Evan Morikawa, Alec Radford, Matthew Knight, Miles Brundage, Mira Murati, Katie Mayer, Peter Welinder, Bob McGrew, Dario Amodei, Sam McCandlish, Ilya Sutskever, and Wojciech Zaremba. Evaluating large language models trained on code, 2021.

Qian Chen, Zhu Zhuo, and Wen Wang. Bert for joint intent classification and slot filling. *arXiv preprint arXiv:1902.10909*, 2019.

Karl Cobbe, Vineet Kosaraju, Mohammad Bavarian, Mark Chen, Heewoo Jun, Lukasz Kaiser, Matthias Plappert, Jerry Tworek, Jacob Hilton, Reiichiro Nakano, Christopher Hesse, and John Schulman. Training verifiers to solve math word problems. *arXiv preprint arXiv:2110.14168*, 2021.

Henry Cunningham, Ryan Huben, et al. Sparse autoencoders find highly interpretable features in language models. In *ICLR*, 2024. URL https://proceedings.iclr.cc/paper_files/paper/2024/file/1fa1ab11f4bd5f94b2ec20e794dbfa3b-Paper-Conference.pdf.

Abhimanyu Dubey, Abhinav Jauhri, Abhinav Pandey, Abhishek Kadian, Ahmad Al-Dahle, Aiesha Letman, Akhil Mathur, Alan Schelten, Amy Yang, Angela Fan, et al. The llama 3 herd of models. *arXiv e-prints*, pp. arXiv–2407, 2024.

Nelson Elhage, Tristan Hume, Catherine Olsson, Nicholas Schiefer, Tom Henighan, Shauna Kravec, Zac Hatfield-Dodds, Robert Lasenby, Dawn Drain, Carol Chen, et al. Toy models of superposition. *arXiv preprint arXiv:2209.10652*, 2022.

Leo Gao, Tom Dupré la Tour, Henk Tillman, Gabriel Goh, Rajan Troll, Alec Radford, Ilya Sutskever, Jan Leike, and Jeffrey Wu. Scaling and evaluating sparse autoencoders, 2024. URL https://cdn.openai.com/papers/sparse-autoencoders.pdf.

Luyu Gao, Aman Madaan, Shuyan Zhou, Uri Alon, Pengfei Liu, Yiming Yang, Jamie Callan, and Graham Neubig. Pal: Program-aided language models. In *International Conference on Machine Learning*, pp. 10764–10799. PMLR, 2023.

Chih-Wen Goo, Guang Gao, Yun-Kai Hsu, Chih-Li Huo, Tsung-Chieh Chen, Keng-Wei Hsu, and Yun-Nung Chen. Slot-gated modeling for joint slot filling and intent prediction. In *Proceedings of the 2018 Conference of the North American Chapter of the Association for Computational Linguistics: Human Language Technologies, Volume 2 (Short Papers)*, pp. 753–757, 2018.

Chuan Guo, Geoff Pleiss, Yu Sun, and Kilian Q Weinberger. On calibration of modern neural networks. In *International conference on machine learning*, pp. 1321–1330. PMLR, 2017.

Daya Guo, Qihao Zhu, Dejian Yang, Zhenda Xie, Kai Dong, Wentao Zhang, Guanting Chen, Xiao Bi, Yu Wu, YK Li, et al. Deepseek-coder: When the large language model meets programming–the rise of code intelligence. *arXiv preprint arXiv:2401.14196*, 2024.

Homa B Hashemi, Amir Asiaee, and Reiner Kraft. Query intent detection using convolutional neural networks. In *International conference on web search and data mining, workshop on query understanding*, volume 23, 2016.

Soufiane Hayou, Nikhil Ghosh, and Bin Yu. Plop: Precise lora placement for efficient finetuning of large models, 2025. URL https://arxiv.org/abs/2506.20629.

Changai He, Sibao Chen, Shilei Huang, Jian Zhang, and Xiao Song. Using convolutional neural network with bert for intent determination. In *2019 International Conference on Asian Language Processing (IALP)*, pp. 65–70. IEEE, 2019.

Dan Hendrycks, Collin Burns, Steven Basart, Andrew Critch, Jerry Li, Dawn Song, and Jacob Steinhardt. Aligning ai with shared human values. *Proceedings of the International Conference on Learning Representations (ICLR)*, 2021a.

Dan Hendrycks, Collin Burns, Steven Basart, Andy Zou, Mantas Mazeika, Dawn Song, and Jacob Steinhardt. Measuring massive multitask language understanding. *Proceedings of the International Conference on Learning Representations (ICLR)*, 2021b.

Dan Hendrycks, Collin Burns, Saurav Kadavath, Akul Arora, Steven Basart, Eric Tang, Dawn Song, and Jacob Steinhardt. Measuring mathematical problem solving with the math dataset. *arXiv preprint arXiv:2103.03874*, 2021c.

John Hewitt and Christopher D Manning. A structural probe for finding syntax in word representations. In *Proceedings of the 2019 Conference of the North American Chapter of the Association for Computational Linguistics: Human Language Technologies, Volume 1 (Long and Short Papers)*, pp. 4129–4138, 2019.

Taesuk Hong, Youbin Ahn, Dongkyu Lee, Joongbo Shin, Seungpil Won, Janghoon Han, Stanley Jungkyu Choi, and Jungyun Seo. Exploring the use of natural language descriptions of intents for large language models in zero-shot intent classification. In *Proceedings of the 25th Annual Meeting of the Special Interest Group on Discourse and Dialogue*, pp. 458–465, 2024.

Ting Jiang, Shaohan Huang, Zhongzhi Luan, Deqing Wang, and Fuzhen Zhuang. Scaling sentence embeddings with large language models. In *EMNLP (Findings)*, pp. 3182–3196, 2024. URL https://aclanthology.org/2024.findings-emnlp.181.

Shibo Jie, Yehui Tang, Kai Han, Zhi-Hong Deng, and Jing Han. Specache: Speculative key-value caching for efficient generation of llms. *arXiv preprint arXiv:2503.16163*, 2025.

Stefan Larson, Anish Mahendran, Joseph J Peper, Christopher Clarke, Andrew Lee, Parker Hill, Jonathan K Kummerfeld, Kevin Leach, Michael A Laurenzano, Lingjia Tang, et al. An evaluation dataset for intent classification and out-of-scope prediction. *arXiv preprint arXiv:1909.02027*, 2019.

Chankyu Lee, Rajarshi Roy, Mengyao Xu, Jonathan Raiman, Mohammad Shoeybi, Bryan Catanzaro, and Wei Ping. Nv-embed: Improved techniques for training llms as generalist embedding models. *arXiv preprint arXiv:2405.17428*, 2024.

Erich Leo Lehmann and George Casella. *Theory of point estimation*. Springer, 1998.

Erich Leo Lehmann and Henry Scheffé. Completeness, similar regions, and unbiased estimation-part i. In *Selected works of EL Lehmann*, pp. 233–268. Springer, 2011.

Quentin Lhoest, Albert Villanova del Moral, Yacine Jernite, Abhishek Thakur, Patrick von Platen, Suraj Patil, Julien Chaumond, Mariama Drame, Julien Plu, Lewis Tunstall, Joe Davison, Mario Šaško, Gunjan Chhablani, Bhavitvya Malik, Simon Brandeis, Teven Le Scao, Victor Sanh, Canwen Xu, Nicolas Patry, Angelina McMillan-Major, Philipp Schmid, Sylvain Gugger, Clément Delangue, Théo Matussière, Lysandre Debut, Stas Bekman, Pierric Cistac, Thibault Goehringer, Victor Mustar, François Lagunas, Alexander Rush, and Thomas Wolf. Datasets: A community library for natural language processing. In *Proceedings of the 2021 Conference on Empirical Methods in Natural Language Processing: System Demonstrations*, pp. 175–184, Online and Punta Cana, Dominican Republic, November 2021. Association for Computational Linguistics. URL https://aclanthology.org/2021.emnlp-demo.21.

Yujia Li, David Choi, Junyoung Chung, Nate Kushman, Julian Schrittwieser, Rémi Leblond, Tom Eccles, James Keeling, Felix Gimeno, Agustin Dal Lago, et al. Competition-level code generation with alphacode. *Science*, 378(6624):1092–1097, 2022.

Hunter Lightman, Vineet Kosaraju, Yura Burda, Harri Edwards, Bowen Baker, Teddy Lee, Jan Leike, John Schulman, Ilya Sutskever, and Karl Cobbe. Let's verify step by step. *arXiv preprint arXiv:2305.20050*, 2023.

Haokun Liu, Derek Tam, Mohammed Muqeeth, Jay Mohta, Tenghao Huang, Mohit Bansal, and Colin A Raffel. Few-shot parameter-efficient fine-tuning is better and cheaper than in-context learning. *Advances in Neural Information Processing Systems*, 35:1950–1965, 2022.

Junhua Liu, Yong Keat Tan, Bin Fu, and Kwan Hui Lim. Balancing accuracy and efficiency in multi-turn intent classification for llm-powered dialog systems in production. *arXiv preprint arXiv:2411.12307*, 2024.

Pengfei Liu, Weizhe Yuan, Jinlan Fu, Zhengbao Jiang, Hiroaki Hayashi, and Graham Neubig. Pre-train, prompt, and predict: A systematic survey of prompting methods in natural language processing. *ACM computing surveys*, 55(9):1–35, 2023.

Xueguang Ma, Liang Wang, Nan Yang, Furu Wei, and Jimmy Lin. Fine-tuning llama for multi-stage text retrieval. In *Proceedings of the 47th International ACM SIGIR Conference on Research and Development in Information Retrieval*, pp. 2421–2425, 2024.

Rui Meng, Ye Liu, Shafiq Rayhan Joty, Caiming Xiong, Yingbo Zhou, and Semih Yavuz. Sfrembedding-mistral: enhance text retrieval with transfer learning. *Salesforce AI Research Blog*, 3:6, 2024.

Niklas Muennighoff. Sgpt: Gpt sentence embeddings for semantic search. *arXiv preprint arXiv:2202.08904*, 2022.

Niklas Muennighoff, SU Hongjin, Liang Wang, Nan Yang, Furu Wei, Tao Yu, Amanpreet Singh, and Douwe Kiela. Generative representational instruction tuning. In *The Thirteenth International Conference on Learning Representations*, 2024.

Arvind Neelakantan, Tao Xu, Raul Puri, Alec Radford, Jesse Michael Han, Jerry Tworek, Qiming Yuan, Nikolas Tezak, Jong Wook Kim, Chris Hallacy, et al. Text and code embeddings by contrastive pre-training. *arXiv preprint arXiv:2201.10005*, 2022.

Zhijie Nie, Zhangchi Feng, Mingxin Li, Cunwang Zhang, Yanzhao Zhang, Dingkun Long, and Richong Zhang. When text embedding meets large language model: a comprehensive survey. *arXiv preprint arXiv:2412.09165*, 2024.

OpenAI. Gpt-5 system card. 2025. URL https://cdn.openai.com/gpt-5-system-card.pdf.

Nina Panickssery, Nick Gabrieli, Julian Schulz, Meg Tong, Evan Hubinger, and Alexander Matt Turner. Steering llama 2 via contrastive activation addition. *arXiv preprint arXiv:2312.06681*, 2023.

Alec Radford, Jeffrey Wu, Rewon Child, David Luan, Dario Amodei, Ilya Sutskever, et al. Language models are unsupervised multitask learners. *OpenAI blog*, 1(8):9, 2019.

Colin Raffel, Noam Shazeer, Adam Roberts, Katherine Lee, Sharan Narang, Michael Matena, Yanqi Zhou, Wei Li, and Peter J Liu. Exploring the limits of transfer learning with a unified text-to-text transformer. *Journal of machine learning research*, 21(140):1–67, 2020.

Juan A Rodriguez, Nicholas Botzer, David Vazquez, Christopher Pal, Marco Pedersoli, and Issam Laradji. Intentgpt: Few-shot intent discovery with large language models. *arXiv preprint arXiv:2411.10670*, 2024.

Noam Shazeer. Fast transformer decoding: One write-head is all you need. *arXiv preprint arXiv:1911.02150*, 2019.

Shivalika Singh, Freddie Vargus, Daniel Dsouza, Börje F. Karlsson, Abinaya Mahendiran, Wei-Yin Ko, Herumb Shandilya, Jay Patel, Deividas Mataciunas, Laura OMahony, Mike Zhang, Ramith Hettiarachchi, Joseph Wilson, Marina Machado, Luisa Souza Moura, Dominik Krzemiński, Hakimeh Fadaei, Irem Ergün, Ifeoma Okoh, Aisha Alaagib, Oshan Mudannayake, Zaid Alyafeai, Vu Minh Chien, Sebastian Ruder, Surya Guthikonda, Emad A. Alghamdi, Sebastian Gehrmann, Niklas Muennighoff, Max Bartolo, Julia Kreutzer, Ahmet Üstün, Marzieh Fadaee, and Sara Hooker. Aya dataset: An open-access collection for multilingual instruction tuning, 2024.

Adnane Souha, Charaf Ouaddi, Lamya Benaddi, and Abdeslam Jakimi. Pre-trained models for intent classification in chatbot: Comparative study and critical analysis. In *2023 6th international conference on advanced communication technologies and networking (CommNet)*, pp. 1–6. IEEE, 2023.

Yixuan Tang and Yi Yang. Pooling and attention: What are effective designs for llm-based embedding models? *arXiv preprint arXiv:2409.02727*, 2024.

Chongyang Tao, Tao Shen, Shen Gao, Junshuo Zhang, Zhen Li, Kai Hua, Wenpeng Hu, Zhengwei Tao, and Shuai Ma. Llms are also effective embedding models: An in-depth overview. *arXiv preprint arXiv:2412.12591*, 2024.

Alexander Matt Turner, Lisa Thiergart, Gavin Leech, David Udell, Juan J Vazquez, Ulisse Mini, and Monte MacDiarmid. Activation addition: Steering language models without optimization. *arXiv e-prints*, pp. arXiv–2308, 2023.

Liang Wang, Nan Yang, Xiaolong Huang, Linjun Yang, Rangan Majumder, and Furu Wei. Improving text embeddings with large language models. In *ACL (1)*, pp. 11897–11916, 2024. URL https://doi.org/10.18653/v1/2024.acl-long.642.

Zhiqiang Wang, Yiran Pang, and Yanbin Lin. Large language models are zero-shot text classifiers. *arXiv preprint arXiv:2312.01044*, 2023.

Jason Wei, Xuezhi Wang, Dale Schuurmans, Maarten Bosma, Fei Xia, Ed Chi, Quoc V Le, Denny Zhou, et al. Chain-of-thought prompting elicits reasoning in large language models. *Advances in neural information processing systems*, 35:24824–24837, 2022.

Yuxiang Wei, Zhe Wang, Jiawei Liu, Yifeng Ding, and Lingming Zhang. Magicoder: Empowering code generation with oss-instruct. *arXiv preprint arXiv:2312.02120*, 2023.

An Yang, Anfeng Li, Baosong Yang, Beichen Zhang, Binyuan Hui, Bo Zheng, Bowen Yu, Chang Gao, Chengen Huang, Chenxu Lv, et al. Qwen3 technical report. *arXiv preprint arXiv:2505.09388*, 2025.

Shunyu Yao, Dian Yu, Jeffrey Zhao, Izhak Shafran, Tom Griffiths, Yuan Cao, and Karthik Narasimhan. Tree of thoughts: Deliberate problem solving with large language models. *Advances in neural information processing systems*, 36:11809–11822, 2023.

Qihao Zhu, Daya Guo, Zhihong Shao, Dejian Yang, Peiyi Wang, Runxin Xu, Y Wu, Yukun Li, Huazuo Gao, Shirong Ma, et al. Deepseek-coder-v2: Breaking the barrier of closed-source models in code intelligence. *arXiv preprint arXiv:2406.11931*, 2024.

A Additional Theoretical Analysis

A.1 Two endpoints on the compression ladder

For each class $k \in [m]$, per-class baselines are computed at the same module W_ℓ on calibration data. We compare the two methods in terms of FLOPs and memory.

VecStat. Method 1: Compute $(S_{\text{vec}}, Q_{\text{vec}})$ as in (1). With per-class parameters $(\mu_k, \Sigma_k = \text{Diag}(\sigma_{k,1}^2, \ldots, \sigma_{k,d}^2))$. The log-likelihood ratio (LLR) between classes i and j is

$$\log \frac{p_i(Y)}{p_j(Y)} = -\frac{T}{2} \sum_{m=1}^{d} \left[\log \frac{\sigma_{i,m}^2}{\sigma_{j,m}^2} + \frac{Q_{\text{vec},m} - 2\mu_{i,m} S_{\text{vec},m} + \mu_{i,m}^2}{\sigma_{i,m}^2} - \frac{Q_{\text{vec},m} - 2\mu_{j,m} S_{\text{vec},m} + \mu_{j,m}^2}{\sigma_{j,m}^2} \right], \tag{4}$$

which is equivalently the average of coordinate-wise Gaussian KLs (since Σ_k is diagonal):

$$\sum_{m=1}^{d} \text{KL}\big(\mathcal{N}(\mu_{i,m}, \sigma_{i,m}^2) \,\|\mathcal{N}(\mu_{j,m}, \sigma_{j,m}^2)\big) = \frac{1}{2} \sum_{m=1}^{d} \left[\log \frac{\sigma_{j,m}^2}{\sigma_{i,m}^2} + \frac{\sigma_{i,m}^2 + (\mu_{i,m} - \mu_{j,m})^2}{\sigma_{j,m}^2} - 1 \right]. \tag{5}$$

Method 2: Using S_{vec}, classify via

$$\cos_k(S_{\text{vec}}, \mu_k) = \frac{\langle S_{\text{vec}}, \mu_k \rangle}{\|S_{\text{vec}}\| \|\mu_k\|}, \qquad \hat{b} = \arg\max_{k \in [m]} \cos_k(S_{\text{vec}}, \mu_k).$$

Costs: *Per-token compute:* $\Theta(d)$. *Prompt-state:* $O(d)$. *Baseline storage:* $O(md)$ numbers. (If only cosine scoring is used, Q_{vec} need not be stored.)

NormStat. Method: Compute $(S_{\text{norm}}, Q_{\text{norm}})$ as in (2), then compare $(S_{\text{norm}}, Q_{\text{norm}})$ to per-class baselines $(\mu_{x,k}, \sigma_{x,k}^2)$ via a 1D Gaussian KL:

$$\text{KL}\big(\mathcal{N}(\mu_{x,i}, \sigma_{x,i}^2) \| \mathcal{N}(\mu_{x,j}, \sigma_{x,j}^2)\big) = \frac{1}{2} \left[\log \frac{\sigma_{x,j}^2}{\sigma_{x,i}^2} + \frac{\sigma_{x,i}^2 + (\mu_{x,i} - \mu_{x,j})^2}{\sigma_{x,j}^2} - 1 \right]. \tag{6}$$

Cost. *Per-token compute:* $\Theta(d)$. *Prompt-state:* $O(1)$. *Baseline storage:* $O(m)$ scalars.

A.2 Sufficiency

We establish the minimal sufficiency of $(S_{\text{vec}}, Q_{\text{vec}})$ for the diagonal–Gaussian model, which is a classical result, see (Lehmann & Casella, 1998; Lehmann & Scheffé, 2011). Intuitively, a sufficient statistic is a lossless compression for inference about the unknown class/parameters: once $(S_{\text{vec}}, Q_{\text{vec}})$ is known, the raw sample Y contains no further information. Minimal sufficiency means no additional compression is possible without losing information—every other sufficient statistic is a measurable function of $(S_{\text{vec}}, Q_{\text{vec}})$.

Lemma 1. *Under* (3) *with diagonal* Σ_k*, the pair* $(S_{\text{vec}}, Q_{\text{vec}})$ *is a* minimal sufficient statistic *for the family* $\{\mathcal{N}(\mu_k, \Sigma_k)^{\otimes T}\}$*, and the class LLR* (4) *depends on the data only through* $(S_{\text{vec}}, Q_{\text{vec}})$.

The proof is provided in Appendix B.

B Proofs

B.1 Proof of Lemma 1

Proof of Lemma 1. Let $Y \coloneqq (y_1, \ldots, y_T) \in \mathbb{R}^{T \times d}$. For a class k, let

$$\theta_k = (\mu_k, \sigma_{k,1}^2, \ldots, \sigma_{k,d}^2), \qquad \Sigma_k = \text{Diag}(\sigma_{k,1}^2, \ldots, \sigma_{k,d}^2).$$

Define the token-wise *sums*

$$S \coloneqq \sum_{t=1}^{T} y_t \in \mathbb{R}^d, \qquad Q \coloneqq \sum_{t=1}^{T} \big(y_t \odot y_t\big) \in \mathbb{R}^d,$$

and write $S_m \coloneqq \sum_{t=1}^{T} y_{t,m}$, $Q_m \coloneqq \sum_{t=1}^{T} y_{t,m}^2$ for coordinates $m = 1, \dots, d$. These relate to the averaged statistics in (1) as follows:

$$S = TS_{\mathrm{vec}}, \qquad Q = (T-1)Q_{\mathrm{vec}} + T\big(S_{\mathrm{vec}} \odot S_{\mathrm{vec}}\big)$$

Since (minimal) sufficiency is invariant under invertible reparameterizations of the statistic, we may work with (S, Q) and translate back to $(S_{\mathrm{vec}}, Q_{\mathrm{vec}})$ via the identities above.

Sufficiency. By (3), y_t are i.i.d. with density

$$p_{\theta_k}(y) = \frac{1}{(2\pi)^{d/2} \prod_{m=1}^{d} \sigma_{k,m}} \exp\left(-\frac{1}{2} \sum_{m=1}^{d} \frac{(y_m - \mu_{k,m})^2}{\sigma_{k,m}^2}\right).$$

Hence the joint density of Y under class k is

$$\begin{aligned} p_{\theta_k}(Y) &= \frac{1}{(2\pi)^{Td/2} \prod_{m=1}^{d} \sigma_{k,m}^{T}} \exp\left(-\frac{1}{2} \sum_{t=1}^{T} \sum_{m=1}^{d} \frac{(y_{t,m} - \mu_{k,m})^2}{\sigma_{k,m}^2}\right) \\ &= \underbrace{\frac{1}{(2\pi)^{Td/2}}}_{\coloneqq h(Y)} \cdot \underbrace{\frac{1}{\prod_{m=1}^{d} \sigma_{k,m}^{T}} \exp\left(-\frac{1}{2} \sum_{m=1}^{d} \frac{Q_m - 2\mu_{k,m} S_m + T\mu_{k,m}^2}{\sigma_{k,m}^2}\right)}_{\coloneqq g_{\theta_k}(S,Q)}. \end{aligned}$$

Thus $p_{\theta_k}(Y) = h(Y)\, g_{\theta_k}(S, Q)$. By the Neyman–Fisher factorization theorem, (S, Q) is sufficient for θ_k, and hence $(S_{\mathrm{vec}}, Q_{\mathrm{vec}})$ is sufficient by the invertible mapping above.

Minimality. Using the Lehmann–Scheffé characterization: a statistic $T(Y)$ is minimal sufficient iff for any Y, Y' the likelihood ratio $p_\theta(Y)/p_\theta(Y')$ is free of θ if and only if $T(Y) = T(Y')$. For our family,

$$\frac{p_\theta(Y)}{p_\theta(Y')} = \exp\left(-\frac{1}{2} \sum_{m=1}^{d} \frac{(Q_m - Q'_m) - 2\mu_m (S_m - S'_m)}{\sigma_m^2}\right).$$

If $(S, Q) = (S', Q')$ then this ratio equals 1, hence is parameter–free. Conversely, if for some m either $S_m \neq S'_m$ or $Q_m \neq Q'_m$, the exponent depends on μ_m (when $S_m \neq S'_m$) or on σ_m^2 (when $Q_m \neq Q'_m$); thus the ratio cannot be constant in θ.

Moreover, for classes i and j, subtracting the two log-likelihoods above yields

$$\log \frac{p_i(Y)}{p_j(Y)} = -\frac{1}{2} \sum_{m=1}^{d} \left(T \log \frac{\sigma_{i,m}^2}{\sigma_{j,m}^2} + \frac{Q_m - 2\mu_{i,m} S_m + T\mu_{i,m}^2}{\sigma_{i,m}^2} - \frac{Q_m - 2\mu_{j,m} S_m + T\mu_{j,m}^2}{\sigma_{j,m}^2}\right),$$

which is exactly (4) and depends on Y only through (S, Q), and equivalently only through $(S_{\mathrm{vec}}, Q_{\mathrm{vec}})$ via the identities at the start of the proof.

This establishes that $(S_{\mathrm{vec}}, Q_{\mathrm{vec}})$ is minimal sufficient and that the LLR depends on the sample only through this pair.

□

B.2 Proof of Theorem 1

Proof of Theorem 1. **Directional regime:** Since $\|\mu_1\| = \|\mu_2\|$, there exists an orthogonal matrix U with $U\mu_1 = \mu_2$. If $Y \sim \mathcal{N}(\mu_1, \sigma^2 I_d)$ then $UY \sim \mathcal{N}(\mu_2, \sigma^2 I_d)$ and $\|UY\| = \|Y\|$. Thus for each t, $\|y_t\| \mid k = 1$ and $\|y_t\| \mid k = 2$ have the same distribution, and by independence the vectors $(\|y_t\|)_{t=1}^{T} \mid k = 1$ and $(\|y_t\|)_{t=1}^{T} \mid k = 2$ are identically distributed. With a uniform prior, any decision rule that depends only on $\{\|y_t\|\}$ has the same acceptance probability under both classes, so its Bayes error is $1/2$.

For the log-likelihood ratio test (LRT), the log-likelihood ratio for two Gaussians with common covariance $\sigma^2 I_d$ is

$$\Lambda(y_{1:T}) = \frac{T}{\sigma^2}\left\langle S_{\text{vec}},\, \mu_1 - \mu_2 \right\rangle - \frac{T}{2\sigma^2}\left(\|\mu_1\|^2 - \|\mu_2\|^2\right).$$

With equal priors the LRT accepts $k = 1$ iff $\Lambda \geq 0$. Under $\|\mu_1\| = \|\mu_2\|$, the constant term vanishes and the decision reduces to the sign of $\langle S_{\text{vec}},\, \mu_1 - \mu_2 \rangle$, i.e., to $\hat{k}$ above.

Let $u \coloneqq (\mu_1 - \mu_2)/\|\mu_1 - \mu_2\|$ and $Z \coloneqq \langle S_{\text{vec}}, u\rangle$. Since $S_{\text{vec}} \mid k \sim \mathcal{N}(\mu_k, \frac{\sigma^2}{T} I_d)$ and $\|u\| = 1$,

$$Z \mid k \sim \mathcal{N}\left(\langle \mu_k, u\rangle,\, \frac{\sigma^2}{T}\right), \quad \langle \mu_1, u\rangle = \tfrac{1}{2}\|\mu_1 - \mu_2\|, \;\; \langle \mu_2, u\rangle = -\tfrac{1}{2}\|\mu_1 - \mu_2\|.$$

Hence, by symmetry,

$$\Pr\left(\hat{k}(y_{1:T}) \neq k\right) = \Pr_{k=1}(Z < 0) = \Phi\left(-\frac{\|\mu_1 - \mu_2\|}{2\sigma}\sqrt{T}\right) \leq \exp\left(-\frac{T}{8\sigma^2}\,\|\mu_1 - \mu_2\|^2\right),$$

where Φ is the standard normal CDF and the last step uses $\Phi(-x) \leq e^{-x^2/2}$ for $x \geq 0$.

Isotropic-scale regime. Let $\phi_d(\,\cdot\,; m, \Sigma)$ denote the d-variate Gaussian density. For $k \in \{1, 2\}$, the *joint* density of $y_{1:T}$ under class k is $p_k(y_{1:T}) \coloneqq \prod_{t=1}^{T} \phi_d\left(y_t; 0, \sigma_k^2 I_d\right)$.

With $\mu_1 = \mu_2 = 0$, $\Sigma_k = \sigma_k^2 I_d$, and $R_T = \sum_{t=1}^{T} \|y_t\|^2$, one can calculate the log-likelihood ratio

$$\log \frac{p_1(y_{1:T})}{p_2(y_{1:T})} = \sum_{t=1}^{T} \log \frac{\phi_d(y_t; 0, \sigma_1^2 I_d)}{\phi_d(y_t; 0, \sigma_2^2 I_d)} = \frac{dT}{2}\log\frac{\sigma_2^2}{\sigma_1^2} + \frac{1}{2}\left(\frac{1}{\sigma_2^2} - \frac{1}{\sigma_1^2}\right) R_T.$$

The right-hand side is an affine (hence strictly monotone when $\sigma_1 \neq \sigma_2$) function of R_T. By the Neyman–Pearson lemma, any Bayes–optimal test is a threshold on R_T, so purely radial statistics are sufficient for optimality and coordinate-wise additions cannot lower the Bayes risk. □

B.3 Proof of Theorem 2

Theorem 3. *Fix a class k. Let $y_1, \ldots, y_N \overset{\text{i.i.d.}}{\sim} \mathcal{N}(\mu_k, \Sigma_k)$ in $\mathbb{R}^d$, where N is the number of calibration samples drawn for this class. Define*

$$\hat{\mu}_k \coloneqq \frac{1}{N}\sum_{i=1}^{N} y_i, \quad \hat{q} \coloneqq \frac{1}{N}\sum_{i=1}^{N} \|y_i\|^2, \quad \sigma_{\max}^2 \coloneqq \|\Sigma_k\|_{\text{op}}.$$

For coordinate variances, write $\sigma_{k,j}^2 \coloneqq (\Sigma_k)_{jj}$ and $\widehat{\sigma}_{k,j}^2 \coloneqq \frac{1}{N}\sum_{i=1}^{N}(y_{i,j} - \hat{\mu}_{k,j})^2,\ j = 1, \ldots, d$. Then:

1. ***NormStat (dimension-free).*** *For $q = \|y\|^2$, one has*

$$\mathbb{E}[q] = \|\mu_k\|^2 + \operatorname{Tr}(\Sigma_k), \quad \operatorname{Var}(q) = 2\operatorname{Tr}(\Sigma_k^2) + 4\mu_k^{\top}\Sigma_k\mu_k.$$

By Bernstein's inequality for sub-exponential variables, for all $\delta \in (0, 1)$,

$$|\hat{q} - q| \lesssim \sqrt{\frac{\operatorname{Var}(q)\log(1/\delta)}{N}} \quad \textit{with probability at least } 1 - \delta.$$

Normalizing by d makes the bound $O(\sqrt{\log(1/\delta)/N})$, i.e. dimension-free.

2. ***VecStat (dimension-dependent).*** *With probability at least $1 - \delta$,*

$$\|\hat{\mu}_k - \mu_k\|_2 \leq C_1\sigma_{\max}\sqrt{\frac{d + \log(1/\delta)}{N}}, \quad \max_j \left|\widehat{\sigma}_{k,j}^2 - \sigma_{k,j}^2\right| \leq C_2\sigma_{\max}^2\sqrt{\frac{\log(d/\delta)}{N}},$$

for absolute constants C_1, C_2. To keep LLR plug-in error small of order ϵ, one needs $N = \Omega(d/\epsilon_\mu^2)$ for mean accuracy in ℓ_2 and $N = \Omega(\log d/\epsilon_\sigma^2)$ for variances in ℓ_∞.

Proof of Theorem 2. **NormStat:** Denote $q_i := \|y_i\|^2$ and $Z_i := q_i - \mathbb{E}[q]$, so that $\hat{q} - \mathbb{E}[q] = \frac{1}{N}\sum_{i=1}^{N} Z_i$. For $y_i \sim \mathcal{N}(\mu_k, \Sigma_k)$, the centered quadratic form Z_i obeys the Hanson–Wright tail bound: there exist absolute constants $c_1, c_2 > 0$ such that for all $t > 0$,

$$\Pr\left(|Z_i| \geq t\right) \;\leq\; 2\exp\left[-\,c_1\,\min\left(\frac{t^2}{\mathrm{Var}(q)},\;\frac{t}{B}\right)\right], \tag{7}$$

where $\mathrm{Var}(q) = 2\,\mathrm{Tr}(\Sigma_k^2) + 4\,\mu_k^\top \Sigma_k \mu_k,\; B = \|\Sigma_k\|_{\mathrm{op}} + \|\mu_k\|^2$. From (7), the Z_i are i.i.d. mean-zero sub-exponential. A standard Bernstein inequality for sums of independent sub-exponential variables then yields, for some absolute $c > 0$ and all $t > 0$,

$$\Pr\left(\left|\frac{1}{N}\sum_{i=1}^{N} Z_i\right| \geq t\right) \leq 2\exp\left[-\,cN\,\min\left(\frac{t^2}{\mathrm{Var}(q)},\;\frac{t}{B}\right)\right].$$

Choosing $t \lesssim \mathrm{Var}(q)/B$ and inverting the tail gives, for any $\delta \in (0,1)$,

$$|\hat{q} - \mathbb{E}[q]| \;\lesssim\; \sqrt{\frac{\mathrm{Var}(q)\log(2/\delta)}{N}} \quad \text{with probability at least } 1-\delta.$$

Since under bounded eigenvalues $\mathrm{Var}(q) = \Theta(d)$, dividing by d yields $\left|\frac{1}{d}\hat{q} - \frac{1}{d}\mathbb{E}[q]\right| \lesssim \sqrt{\frac{\log(2/\delta)}{N}}$, which is dimension-free.

VecStat: Let $z_i := \Sigma_k^{-1/2}(y_i - \mu_k) \sim \mathcal{N}(0, I_d)$. Then

$$\hat{\mu}_k - \mu_k = \Sigma_k^{1/2}\left(\frac{1}{N}\sum_{i=1}^{N} z_i\right) \sim \mathcal{N}\left(0,\;\frac{1}{N}\Sigma_k\right).$$

Hence, $\|\Sigma_k^{-1/2}(\hat{\mu}_k - \mu_k)\|_2^2 \;\sim\; \frac{1}{N}\chi_d^2$. Recall the standard Laurent-Massart inequalities: for any $x > 0$,

$$\Pr\left(\chi_d^2 - d \geq 2\sqrt{dx} + 2x\right) \leq e^{-x}, \quad \Pr\left(d - \chi_d^2 \geq 2\sqrt{dx}\right) \leq e^{-x}. \tag{8}$$

Applying (8) with $x = \log(1/\delta)$ and scaling by $1/N$ yields, with probability $\geq 1-\delta$,

$$\|\Sigma_k^{-1/2}(\hat{\mu}_k - \mu_k)\|_2 \leq \sqrt{\frac{1}{N}\left(d + 2\sqrt{d\log(1/\delta)} + 2\log(1/\delta)\right)}.$$

Multiplying by $\|\Sigma_k^{1/2}\|_{\mathrm{op}} = \sigma_{\max}$ and using $\sqrt{a+b} \leq \sqrt{a} + \sqrt{b}$ gives

$$\|\hat{\mu}_k - \mu_k\|_2 \leq C_1\sigma_{\max}\sqrt{\frac{d + \log(1/\delta)}{N}},$$

for an absolute constant $C_1 > 0$.

□

C Experiment details

C.1 Dataset composition and processing strategies

Table 4: Datasets composition for level-1 classification.

Category	Calibration Data	# Calibration Samples	Classification Data	# Classification Samples
General Text	MMLU (European History)	165	MMLU (US History)	204
Math	GSM8K	2,000	GSM8K MATH500	1,319 500
Code	Magicoder	2,000	Magicoder HumanEval	5,000 164

We evaluate our lightweight intent classification methods across two hierarchical granularities. Our experimental protocol consists of two stages: calibration and classification. During calibration, we compute per-class baseline statistics (NormStat or VecStat) from calibration data passed through pretrained LLMs. During classification, we compute the same statistics for test prompts and assign labels based on the minimum KL divergence (or cosine distance) between the prompt's statistics and the calibrated per-class baselines.

Table 5: Datasets composition for level-2 classification.

Task	Data Source	Classes	# Calibration Samples per Class	# Classification Samples per Class
Code	Magicoder	C++, C#, Java, PHP, Python, Rust, Shell, Swift, TypeScript	2000	5000
Math	Competition Math	Algebra, Counting & Probability, Geometry, Intermediate Algebra, Number Theory, Prealgebra, Precalculus	800	3000
Natural Language	Aya	Sinhala, Tamil, English, Moroccan Arabic, Japanese	512	3000

Classification granularities We consider the following classification granularities:

- **Level-1 Classification** evaluates coarse-grained categorization into three primary domains: general text, mathematics, and code. This level represents the typical routing scenario where prompts are directed to specialized models based on broad task categories.
- **Level-2 Classification** examines fine-grained discrimination within each domain. We evaluate three distinct tasks: (i) programming language identification across nine languages in code prompts, (ii) mathematical subfield classification across seven topics, and (iii) natural language identification across five linguistically diverse languages.

Datasets and evaluation Table 4 and Table 5 present the complete dataset composition. For Level-1 classification, we calibrate using domain-representative datasets: MMLU European History for general text (165 samples), GSM8K for math (2,000 samples), and Magicoder for code (2,000 samples). Classification evaluation employs both in-distribution and out-of-distribution datasets to assess generalization. Specifically, we evaluate general text on MMLU US History, mathematics on GSM8K (in-distribution) and MATH500 (out-of-distribution), and code on Magicoder (in-distribution) and HumanEval (out-of-distribution).

For Level-2 classification, we maintain consistent calibration sizes where feasible: 2,000 samples per programming language, 800 samples per mathematical subfield, and 512 samples per natural language. Classification sets contain up to 5,000 samples per programming language and 3,000 samples per category for mathematics and natural languages, subject to dataset availability. We also provide more details on the datasets used in Appendix C.2.

C.2 Datasets

We employ seven benchmark datasets spanning general text, mathematics, and code domains to evaluate intent classification performance at both granularity levels.

- **General Text Datasets**. For Level-1 evaluation, we utilize MMLU (Hendrycks et al., 2021a;b), a comprehensive benchmark of multiple-choice questions across 57 subjects. We construct calibration data using the High School European History subset and evaluate on the High School US History subset, using question-choice pairs as input. For Level-2 language classification, we employ the Aya dataset (Singh et al., 2024), which contains human-annotated prompts across 65 languages. We select five linguistically diverse languages as specified in Table 5 and use the input field for classification.
- **Mathematics Datasets**. We employ three mathematics benchmarks for comprehensive evaluation. GSM8K (Cobbe et al., 2021) provides grade-school word problems requiring multi-step reasoning, from which we sample 2,000 calibration instances and use the complete test set for Level-1 classification. MATH500 (Lightman et al., 2023) serves as an out-of-distribution test set containing 500 problems from the MATH benchmark. For Level-2 domain-specific classification, Competition Math (Hendrycks et al., 2021c) provides problems from mathematics competitions spanning seven mathematical subfields including algebra, geometry, and number theory. We use the problem field as model input for Level-2 domain-specific classification.
- **Code Datasets**. Magicoder (Wei et al., 2023) forms our primary code classification resource, containing solutions across multiple programming languages. We utilize the solution field as

model input for both Level-1 general code classification and Level-2 language-specific classification tasks, focusing on 9 mainstream programming languages as detailed in Table 5. HumanEval (Chen et al., 2021) provides 164 function-level programming problems, where we use the prompt field containing function signatures and docstrings as model input, serving as an out-of-distribution test set for Level-1 classification.

All datasets are publicly available through HuggingFace Datasets (Lhoest et al., 2021). The exact sampling strategies and train-test splits follow the specifications in Table 4 and Table 5, with test samples capped at the minimum of specified counts and available data.

C.3 Selected LLMs

We evaluate our approach on 7 pretrained large language models spanning 1B to 32B parameters, encompassing both base and instruction-tuned variants. This selection provides comprehensive coverage across model scales and training stages. We consider the following two LLM families:

- **Qwen family** (Yang et al., 2025): We evaluate four models from the Qwen3 series. The instruction-tuned variants include Qwen3-1.7B (28 layers), Qwen3-4B (36 layers), Qwen3-8B (36 layers), and Qwen3-32B (64 layers), each post-trained with supervised fine-tuning and reinforcement learning from human feedback (RLHF). Additionally, we include Qwen3-1.7B-Base to assess performance on pretrained models without alignment. For all Qwen3 evaluations, we switch on non-thinking mode to ensure consistent comparison across models.
- **Llama family** (Dubey et al., 2024): We evaluate Llama-3.2-1B (16 layers) and its instruction-tuned counterpart Llama-3.2-1B-Instruct. The instruction-tuned variant underwent supervised fine-tuning and RLHF to better align with human preferences.

This benchmark model selection enables systematic evaluation across three critical dimensions: model scale (from 1B to 32B parameters), training paradigm (pretrained-only versus post-trained), and architectural diversity (Qwen and Llama families). The substantial range in model sizes—spanning over an order of magnitude in parameters—allows us to rigorously test whether our method can effectively operate across vastly different computational scales and model capacities. The comparison between base and aligned models reveals how post-training procedures affect our method's performance, demonstrating whether it remains equally effective for both pretrained and instruction-tuned models.

C.4 More Implementation Details

To stabilize training, we normalize input features and weight matrices through the following process:

1. Input Normalization: The input tensor z is normalized to unit norm for stability:
$$z_{\text{normalized}} = \frac{z}{\|z\|_2 + \epsilon}.$$
2. Weight Normalization: The weight matrix W is normalized using its Frobenius norm:
$$W_{\text{normalized}} = \frac{W}{\sqrt{\text{mean}(W^2)} + \epsilon}.$$
3. Activation Computation: The normalized input is multiplied by the normalized weight matrix:
$$Wz = z_{\text{normalized}} \cdot W^T_{\text{normalized}}.$$

The statistics for NormStat and VecStat are computed from Wz. Note that this is likely suboptimal; in a production-scale implementation we should read Wz directly from the module's output rather than recomputing it.

C.5 Pseudo-Algorithm

Our task inference approach follows the following steps:

Algorithm 1 Intent Classification with NormStat or VecStat

Require: Input prompt x, baseline scores $\{S_1, S_2, \ldots, S_m\}$ for tasks $C_1, C_2, \ldots, C_m$, distance function "dist" (NormStat: KL; VecStat: KL or cosine similarity)
Ensure: Predicted task T_{pred} and confidence scores
1: Compute statistic scores S_x from input x
2: **for** each task C_i **do**
3: Compute distance $d_i = \text{dist}(S_x, S_i)$
4: **end for**
5: $C_{\text{pred}} = \arg\min_{C_i} d_i$
6: Compute probabilities via softmax: $p_i = \frac{\exp(-(d_i - \bar{d})/\tau)}{\sum_j \exp(-(d_j - \bar{d})/\tau)}$ (used for uncertainty quantification, $\bar{d}$ is the average, τ is the temperature)
7: **return** $C_{\text{pred}}, \{p_1, p_2, \ldots, p_m\}$

C.6 Hardware and software environment

We conducted experiments on two computational platforms based on model scales. For models up to 4B parameters, we utilized an NVIDIA L40S GPU with 48GB of memory. For larger models (Qwen3-8B and Qwen3-32B), experiments were performed on an NVIDIA Grace Hopper GH200 superchip, featuring a Grace ARM 72-core CPU with 120GB RAM and a NVIDIA H100 GPU with 96GB of memory. All experiments are implemented using Python 3.12.0 and PyTorch 2.7.0 with CUDA 12.6.

D Additional Experimental Results

D.1 Additional Results for Level-1 Classification.

Please refer to Table 6.

D.2 Addtional Results for Level-2 Experiments

For programming languages, please refer to Table 7. For math, please refer to Table 8. For natural languages, refer to Table 9.

D.3 Case Study

Fig. 6 presents the mixed-intent prompt used in Section 3.3, constructed by concatenating code content with mathematical content. We also evaluated the reverse concatenation order (mathematics followed by code), with results shown in Fig. 7. The uncertainty quantification patterns remain consistent across both prompt orderings.

D.4 The effect of the number of layers considered

See Fig. 8.

D.5 Calibration Convergence Analysis

See Fig. 9.

D.6 The effect of the maximum prompt length

See Fig. 10.

Table 6: Level-1 classification results for all seven LLMs.

Model	Method	gsm8k	humaneval	magicoder	math500	mmlu_history
Qwen3-1.7B	Avg-MLP	99.97±0.04	99.80±0.35	99.99±0.02	78.33±1.67	100.00±0.00
	Tail-MLP	100.00±0.00	100.00±0.00	99.97±0.02	99.00±0.00	100.00±0.00
	NormStat:KL	97.35±0.00	70.12±0.61	99.27±0.11	76.60±0.20	100.00±0.00
	VecStat:KL	100.00±0.00	99.39±0.00	99.97±0.03	88.33±0.30	100.00±0.00
	VecStat:Cos	100.00±0.00	98.78±0.00	99.97±0.03	92.26±0.11	100.00±0.00
Qwen3-1.7B-Base	Avg-MLP	78.09±31.54	99.80±0.35	100.00±0.00	40.60±19.91	100.00±0.00
	Tail-MLP	100.00±0.00	84.55±26.76	99.87±0.18	99.00±0.00	100.00±0.00
	NormStat:KL	79.71±0.29	82.93±0.00	99.71±0.03	88.47±0.12	100.00±0.00
	VecStat:KL	40.46±0.10	100.00±0.00	100.00±0.0	49.06±0.95	100.00±0.00
	VecStat:Cos	99.84±0.00	99.39±0.00	99.98±0.02	92.30±0.39	100.00±0.00
Llama-3.2-1B	Avg-MLP	100.00±0.00	100.00±0.00	99.99±0.01	64.33±8.33	99.84±0.28
	Tail-MLP	99.95±0.04	100.00±0.00	99.97±0.03	98.93±0.42	99.35±1.13
	NormStat:KL	99.49±0.09	90.85±0.00	96.39±0.20	83.40±0.00	92.48±0.57
	VecStat:KL	100.00±0.00	99.39±0.00	99.98±0.02	78.80±0.12	100.00±0.00
	VecStat:Cos	100.00±0.00	99.39±0.00	99.97±0.02	77.60±0.20	100.00±0.00
Llama-3.2-1B-Instruct	Avg-MLP	100.00±0.00	99.59±0.35	99.99±0.02	72.40±2.91	100.00±0.00
	Tail-MLP	100.00±0.00	100.00±0.00	99.89±0.05	94.53±0.42	100.00±0.00
	NormStat:KL	100.00±0.00	65.24±0.00	97.21±0.21	96.20±0.00	98.53±0.00
	VecStat:KL	100.00±0.00	99.39±0.00	99.96±0.01	87.87±0.11	100.00±0.00
	VecStat:Cos	100.00±0.00	99.39±0.00	99.97±0.03	85.60±0.00	100.00±0.00
Qwen3-4B	Avg-MLP	99.95±0.09	100.00±0.00	99.99±0.01	79.27±4.39	100.00±0.00
	Tail-MLP	100.00±0.00	100.00±0.00	99.96±0.02	92.27±1.17	100.00±0.00
	NormStat:KL	96.36±0.00	35.57±0.35	99.84±0.03	89.40±0.00	99.84±0.28
	VecStat:KL	99.97±0.04	100.00±0.00	99.99±0.02	91.73±0.23	100.00±0.00
	VecStat:Cos	100.00±0.00	96.34±0.00	99.97±0.03	93.40±0.20	100.00±0.00
Qwen3-8B	Avg-MLP	99.42±0.74	99.59±0.35	99.99±0.02	77.27±11.02	100.00±0.00
	Tail-MLP	99.82±0.12	98.58±2.46	99.98±0.02	81.20±9.72	100.00±0.00
	NormStat:KL	85.14±0.35	10.37±1.06	99.85±0.06	92.93±0.12	99.51±0.49
	VecStat:KL	99.95±0.04	99.59±0.35	99.99±0.02	92.20±0.00	100.00±0.00
	VecStat:Cos	100.00±0.00	95.73±0.61	99.98±0.03	94.20±0.00	100.00±0.00
Qwen3-32B	Avg-MLP	95.88±3.31	100.00±0.00	99.99±0.01	86.87±5.22	100.00±0.00
	Tail-MLP	99.39±0.00	100.00±0.00	99.98±0.00	96.80±0.40	99.02±0.49
	NormStat:KL	97.93±0.04	24.59±0.35	99.78±0.06	97.93±0.12	100.00±0.00
	VecStat:KL	100.00±0.00	99.39±0.00	99.98±0.03	96.60±0.00	100.00±0.00
	VecStat:Cos	100.00±0.00	98.17±0.00	99.98±0.03	96.80±0.35	100.00±0.00

Table 7: Level-2 programming language classification results for all seven LLMs. Values represent per-language accuracy across nine programming languages from the Magicoder dataset.

Model	Method	cpp	csharp	java	php	python	rust	shell	swift	typescript
Qwen3-1.7B	Avg-MLP	99.97±0.03	100.00±0.00	100.00±0.00	99.96±0.06	99.89±0.01	100.00±0.00	99.92±0.14	100.00±0.00	99.94±0.07
	Tail-MLP	99.54±0.09	99.57±0.06	99.41±0.26	99.89±0.11	99.35±0.27	99.32±0.17	99.92±0.14	99.81±0.07	99.52±0.03
	NormStat:KL	53.18±0.60	53.17±1.96	40.39±0.63	57.35±1.97	60.17±0.89	58.07±0.55	88.73±1.67	59.47±0.88	49.59±0.34
	VecStat:KL	98.83±0.18	98.98±0.39	98.21±0.15	99.81±0.23	99.06±0.09	99.68±0.14	99.52±0.00	99.81±0.12	99.26±0.20
	VecStat:Cos	98.51±0.19	98.78±0.37	97.79±0.19	99.85±0.17	99.06±0.14	99.35±0.15	99.84±0.14	99.55±0.11	99.02±0.29
Qwen3-1.7B-Base	Avg-MLP	99.97±0.03	99.96±0.04	99.97±0.03	100.00±0.00	99.89±0.05	100.00±0.00	99.92±0.14	100.00±0.00	99.96±0.04
	Tail-MLP	99.28±0.19	99.37±0.19	99.23±0.12	99.96±0.06	99.25±0.14	99.27±0.19	99.84±0.27	99.75±0.14	99.50±0.03
	NormStat:KL	47.76±0.18	43.75±1.18	36.92±0.96	60.44±1.13	56.03±0.82	54.88±0.78	88.33±2.42	57.85±1.25	51.20±0.25
	VecStat:KL	98.29±0.13	98.37±0.53	97.00±0.21	99.66±0.11	98.63±0.09	99.45±0.12	99.68±0.14	99.64±0.12	99.17±0.19
	VecStat:Cos	98.27±0.17	98.23±0.50	96.91±0.05	99.63±0.17	98.84±0.09	99.47±0.13	99.68±0.14	99.58±0.07	98.54±0.30
Llama-3.2-1B	Avg-MLP	99.97±0.03	99.98±0.04	99.97±0.05	99.96±0.06	99.91±0.02	100.00±0.00	100.00±0.00	100.00±0.00	99.94±0.03
	Tail-MLP	99.21±0.24	99.08±0.16	99.41±0.10	99.85±0.17	99.25±0.26	99.21±0.32	99.84±0.27	99.75±0.09	99.58±0.11
	NormStat:KL	44.23±1.37	39.54±2.26	35.09±1.07	49.25±1.60	38.65±0.71	54.91±0.78	90.95±1.56	55.63±1.24	34.67±1.81
	VecStat:KL	98.77±0.19	98.37±0.43	97.14±0.07	99.63±0.17	98.66±0.21	99.79±0.03	99.84±0.27	99.73±0.18	99.02±0.25
	VecStat:Cos	98.53±0.12	97.78±0.25	96.34±0.09	99.52±0.28	98.86±0.18	99.48±0.15	99.60±0.14	99.49±0.25	98.81±0.36
Llama-3.2-1B-Instruct	Avg-MLP	99.95±0.05	99.98±0.04	99.97±0.03	99.96±0.06	99.91±0.01	100.00±0.00	99.92±0.14	100.00±0.00	99.99±0.03
	Tail-MLP	99.07±0.39	99.23±0.15	99.12±0.40	99.55±0.22	99.27±0.11	99.00±0.49	99.84±0.27	99.70±0.16	99.64±0.04
	NormStat:KL	41.34±1.45	45.89±0.57	33.32±1.51	45.23±2.25	46.42±1.32	55.80±0.67	89.76±2.52	57.64±0.72	34.05±2.20
	VecStat:KL	98.56±0.19	97.58±0.19	97.25±0.13	99.70±0.17	98.87±0.16	99.66±0.08	99.84±0.27	99.62±0.14	99.02±0.27
	VecStat:Cos	98.56±0.19	97.46±0.34	96.85±0.23	99.78±0.19	99.00±0.13	99.37±0.10	99.84±0.27	99.64±0.14	98.87±0.32
Qwen3-4B	Avg-MLP	99.97±0.03	99.94±0.00	100.00±0.00	99.96±0.06	99.89±0.01	100.00±0.00	100.00±0.00	100.00±0.00	99.94±0.03
	Tail-MLP	99.37±0.11	99.53±0.13	99.46±0.03	99.81±0.13	99.48±0.02	99.35±0.27	99.84±0.27	99.73±0.14	99.66±0.07
	NormStat:KL	54.55±1.04	40.86±1.39	35.45±0.28	56.26±0.68	69.71±1.04	68.76±0.65	93.10±1.33	72.17±1.20	48.70±0.32
	VecStat:KL	99.26±0.08	98.60±0.38	97.95±0.12	99.74±0.26	99.07±0.09	99.82±0.03	99.76±0.00	99.87±0.12	99.30±0.19
	VecStat:Cos	98.92±0.09	98.86±0.44	98.18±0.05	99.89±0.19	99.13±0.08	99.53±0.10	99.84±0.14	99.79±0.13	99.26±0.23
Qwen3-8B	Avg-MLP	99.95±0.05	100.00±0.00	100.00±0.00	99.96±0.06	99.91±0.01	100.00±0.00	100.00±0.00	100.00±0.00	99.94±0.03
	Tail-MLP	99.61±0.16	99.69±0.18	99.47±0.12	100.00±0.00	99.39±0.22	99.53±0.10	99.92±0.14	99.75±0.07	99.61±0.10
	NormStat:KL	47.37±0.94	38.26±1.28	27.59±0.65	60.14±1.27	67.73±0.54	63.05±0.43	91.51±0.60	62.54±1.25	49.28±0.84
	VecStat:KL	99.09±0.11	98.58±0.42	97.78±0.09	99.78±0.22	99.01±0.04	99.81±0.00	99.76±0.00	99.91±0.09	99.38±0.20
	VecStat:Cos	98.90±0.24	98.96±0.38	98.49±0.03	99.85±0.13	99.13±0.12	99.55±0.07	100.00±0.00	99.81±0.12	99.35±0.19
Qwen3-32B	Avg-MLP	99.91±0.03	99.98±0.04	100.00±0.00	99.96±0.06	99.91±0.03	99.97±0.06	100.00±0.00	100.00±0.00	99.96±0.04
	Tail-MLP	98.01±0.41	97.27±0.95	97.99±0.53	98.77±0.22	98.26±0.21	99.21±0.06	98.97±0.60	98.71±0.48	98.50±0.07
	NormStat:KL	53.57±0.94	36.94±1.38	25.47±1.43	59.47±0.57	61.66±1.40	67.63±0.54	89.29±0.71	69.35±1.19	49.84±1.08
	VecStat:KL	99.01±0.11	99.35±0.34	98.72±0.03	99.89±0.11	99.29±0.06	99.90±0.05	100.00±0.00	99.85±0.09	99.75±0.16
	VecStat:Cos	99.18±0.14	99.53±0.19	99.01±0.10	99.89±0.11	99.50±0.04	99.81±0.13	100.00±0.00	99.87±0.12	99.72±0.09

Table 8: Level-2 mathematical subfield classification results for all seven LLMs. Values represent per-subfield accuracy across seven mathematical subfields from the Competition Math dataset.

Model	Method	Algebra	Counting & Probability	Geometry	Intermediate Algebra	Number Theory	Prealgebra	Precalculus
Qwen3-1.7B	Avg-MLP	71.78±5.57	79.48±1.91	89.98±3.46	79.33±3.96	84.02±2.56	50.00±2.29	82.79±3.37
	Tail-MLP	65.79±3.55	76.10±4.24	84.88±4.43	71.86±6.02	82.32±3.80	50.31±2.59	73.58±4.30
	NormStat:KL	23.67±1.27	37.83±0.65	48.15±4.09	58.75±1.08	65.46±1.25	0.97±0.28	33.88±1.02
	VecStat:KL	33.29±1.39	53.71±2.00	35.88±3.28	81.88±0.58	86.26±0.62	1.46±0.05	46.07±1.82
	VecStat:Cos	57.66±0.70	61.50±2.16	36.07±3.37	73.58±0.83	86.92±0.38	2.22±0.32	51.22±1.61
Qwen3-1.7B-Base	Avg-MLP	67.96±1.83	79.55±0.67	90.53±0.55	83.93±2.34	84.02±2.62	48.85±2.19	83.47±3.46
	Tail-MLP	70.97±4.48	80.97±2.25	90.89±1.14	74.49±2.32	81.50±6.42	51.93±7.96	78.25±2.55
	NormStat:KL	23.35±0.70	37.23±2.12	47.36±4.20	56.65±1.30	58.84±2.38	5.67±2.17	34.82±0.82
	VecStat:KL	39.48±3.28	50.86±1.72	35.88±3.37	81.31±0.65	88.12±0.58	1.52±0.52	46.41±1.24
	VecStat:Cos	61.24±0.90	62.62±2.31	36.00±3.55	73.46±0.80	88.18±0.28	2.66±0.67	53.59±0.82
Llama-3.2-1B	Avg-MLP	57.99±6.53	75.13±5.42	86.22±4.37	75.94±4.00	78.43±0.09	41.67±5.38	76.02±1.42
	Tail-MLP	58.38±4.88	78.35±2.40	91.20±1.28	74.44±3.57	77.45±8.21	36.26±4.71	67.01±5.55
	NormStat:KL	19.46±3.91	16.33±1.35	38.07±2.98	37.01±3.69	80.24±2.55	0.05±0.05	27.71±1.73
	VecStat:KL	34.57±0.92	50.34±1.92	38.19±4.30	76.13±0.97	84.89±0.59	1.38±0.12	48.17±2.66
	VecStat:Cos	44.71±0.78	59.48±2.26	44.63±5.73	72.65±0.35	83.96±1.19	2.30±0.32	52.57±0.92
Llama-3.2-1B-Instruct	Avg-MLP	64.88±4.97	78.95±1.01	86.76±4.30	76.82±5.70	85.39±0.43	45.27±2.58	84.35±2.00
	Tail-MLP	73.63±4.07	79.48±2.60	88.71±2.03	78.02±2.53	83.58±0.16	51.28±3.11	83.47±1.84
	NormStat:KL	4.38±3.24	11.69±1.57	36.13±3.19	37.34±3.24	84.40±1.00	0.26±0.12	27.98±4.39
	VecStat:KL	40.03±2.62	45.09±1.50	35.88±3.46	74.32±1.49	88.67±0.43	1.25±0.14	46.75±2.34
	VecStat:Cos	53.20±1.76	59.85±1.80	36.79±4.02	72.72±1.04	86.59±0.19	1.78±0.09	52.17±1.54
Qwen3-4B	Avg-MLP	73.52±1.54	79.63±4.68	89.80±2.86	79.16±1.48	80.84±0.78	51.23±3.88	84.62±2.94
	Tail-MLP	68.98±9.23	82.47±1.96	82.70±2.37	67.84±7.26	81.55±3.51	46.89±4.30	79.95±1.50
	NormStat:KL	19.57±3.97	17.15±0.91	42.26±3.41	47.00±2.72	76.79±2.63	0.60±0.25	34.28±1.70
	VecStat:KL	29.80±3.56	51.99±1.30	35.82±3.37	82.31±1.15	89.00±0.28	1.36±0.05	54.81±3.00
	VecStat:Cos	62.24±2.09	61.72±2.03	36.13±3.19	73.89±1.24	88.83±0.33	1.96±0.08	53.59±1.32
Qwen3-8B	Avg-MLP	73.94±1.63	82.70±0.98	87.13±0.56	81.00±3.61	86.59±4.35	52.95±5.24	89.36±0.42
	Tail-MLP	68.43±1.81	80.52±2.03	89.92±1.91	73.87±6.12	82.92±5.55	53.58±0.64	81.10±5.72
	NormStat:KL	21.01±6.35	19.03±1.50	40.19±3.56	46.38±0.91	73.45±4.22	0.73±0.59	31.98±1.31
	VecStat:KL	36.23±3.18	51.24±1.17	35.88±3.28	81.00±1.60	88.89±0.47	1.52±0.12	55.15±3.27
	VecStat:Cos	64.46±1.45	61.95±1.87	36.25±3.19	74.13±0.95	89.33±0.33	2.06±0.40	55.08±1.08
Qwen3-32B	Avg-MLP	73.25±4.75	77.83±2.89	89.01±3.74	84.14±3.27	81.88±2.64	57.92±4.22	86.65±3.02
	Tail-MLP	66.70±8.95	78.43±2.02	88.52±4.65	79.61±3.33	74.06±11.10	50.57±10.68	80.62±3.30
	NormStat:KL	31.99±2.02	21.72±0.85	40.56±3.48	44.61±1.14	75.53±2.56	0.13±0.05	31.44±1.47
	VecStat:KL	55.76±1.11	58.50±2.04	35.94±3.28	77.80±1.04	89.87±0.34	1.46±0.12	52.78±0.59
	VecStat:Cos	71.16±0.46	64.42±2.16	37.04±3.20	73.32±0.82	89.49±0.87	3.00±0.72	58.47±1.31

Table 9: Level-2 natural language classification results for all seven LLMs. Values represent per-language accuracy across five natural languages from the Aya dataset.

Model	Method	English	Japanese	Moroccan Arabic	Sinhala	Tamil
Qwen3-1.7B	Avg-MLP	99.74±0.12	99.99±0.02	99.97±0.03	99.99±0.02	99.94±0.04
	Tail-MLP	99.49±0.15	100.00±0.00	99.97±0.03	99.93±0.06	99.94±0.10
	NormStat:KL	82.26±1.39	81.42±0.81	85.78±0.86	99.87±0.12	99.52±0.12
	VecStat:KL	96.27±0.34	99.83±0.03	99.97±0.00	99.99±0.02	99.93±0.06
	VecStat:Cos	98.09±0.10	99.82±0.05	99.99±0.02	99.99±0.02	99.94±0.04
Qwen3-1.7B-Base	Avg-MLP	99.64±0.15	100.00±0.00	99.94±0.04	99.99±0.02	99.96±0.02
	Tail-MLP	99.67±0.12	100.00±0.00	99.97±0.03	99.98±0.02	99.87±0.03
	NormStat:KL	82.58±1.88	83.08±1.35	73.59±0.57	99.83±0.09	98.43±0.17
	VecStat:KL	97.41±0.13	99.84±0.05	99.97±0.03	99.99±0.02	99.93±0.06
	VecStat:Cos	98.46±0.13	99.83±0.09	100.00±0.00	99.99±0.02	99.94±0.04
Llama-3.2-1B	Avg-MLP	99.63±0.21	100.00±0.00	99.97±0.03	99.99±0.02	99.96±0.02
	Tail-MLP	99.60±0.18	100.00±0.00	99.97±0.03	99.87±0.00	99.71±0.28
	NormStat:KL	77.26±6.21	57.36±3.14	98.56±0.11	99.67±0.20	99.82±0.19
	VecStat:KL	96.12±0.39	99.92±0.02	99.96±0.02	100.00±0.00	99.96±0.02
	VecStat:Cos	98.76±0.07	99.98±0.02	99.96±0.02	99.99±0.02	99.94±0.04
Llama-3.2-1B-Instruct	Avg-MLP	99.72±0.10	99.99±0.02	99.94±0.04	99.99±0.02	99.97±0.03
	Tail-MLP	99.58±0.15	100.00±0.00	99.96±0.02	99.94±0.07	99.82±0.20
	NormStat:KL	79.47±5.07	42.79±2.16	98.54±0.18	99.86±0.13	99.86±0.07
	VecStat:KL	96.04±0.39	99.84±0.13	99.98±0.02	99.99±0.02	99.96±0.02
	VecStat:Cos	98.59±0.12	99.98±0.02	99.94±0.04	99.99±0.02	99.94±0.04
Qwen3-4B	Avg-MLP	99.71±0.10	100.00±0.00	99.94±0.04	99.99±0.02	99.96±0.02
	Tail-MLP	99.60±0.15	100.00±0.00	99.97±0.03	99.99±0.02	99.99±0.02
	NormStat:KL	84.60±0.34	90.29±1.27	90.53±0.61	99.84±0.07	99.11±0.54
	VecStat:KL	93.99±0.82	99.77±0.09	100.00±0.00	99.99±0.02	99.93±0.06
	VecStat:Cos	97.73±0.12	99.88±0.10	100.00±0.00	99.99±0.02	99.94±0.04
Qwen3-8B	Avg-MLP	99.70±0.06	100.00±0.00	99.94±0.04	99.99±0.02	99.97±0.00
	Tail-MLP	99.53±0.15	100.00±0.00	99.97±0.03	99.99±0.02	99.92±0.08
	NormStat:KL	85.06±0.85	92.03±1.32	76.76±0.77	99.92±0.04	96.69±2.25
	VecStat:KL	96.27±0.38	99.82±0.05	100.00±0.00	100.00±0.00	99.93±0.06
	VecStat:Cos	98.66±0.13	99.83±0.09	100.00±0.00	99.99±0.02	99.94±0.04
Qwen3-32B	Avg-MLP	0.00±0.00	0.00±0.00	0.00±0.00	100.00±0.00	0.00±0.00
	Tail-MLP	0.00±0.00	0.00±0.00	0.00±0.00	100.00±0.00	0.00±0.00
	NormStat:KL	97.43±0.07	0.00±0.00	0.00±0.00	0.01±0.02	0.00±0.00
	VecStat:KL	97.57±0.10	0.00±0.00	0.00±0.00	0.00±0.00	0.00±0.00
	VecStat:Cos	97.57±0.10	0.00±0.00	0.00±0.00	0.00±0.00	0.00±0.00

Code+Math

```static func calcWidth(text: String) -> CGFloat {
    let constants = StoreSortBaseCell.Constants()
    let textWidth = HelperManager.textWidth(text, font: constants.titleLabelFont)
    return constants.horizontalSpace
        + textWidth
        + constants.spaceBetweenStarAndTitleLabel
        + constants.starImageViewSize
        + constants.spaceBetweenSeparatorAndImageView
        + constants.verticalSeparatorWidth
        + constants.spaceBetweenSeparatorAndImageView
        + constants.dropDownButtonWidth
        + constants.horizontalSpace
} ```

In the solution, the `calcWidth` function takes the input text and calculates the width based on the provided constants and helper function. It first initializes the constants and then uses the `textWidth` helper function to calculate the width of the input text. Finally, it computes the total width based on the constants and returns the result as a floating-point number.

-Jame will turn 27 in 5 years. In 8 years his cousin will be 5 years younger than twice his age. How many years separate the age of the two now?

Figure 6: Mixed-intent prompt example combining Swift code (width calculation function) and a mathematical problem used for uncertainty quantification analysis.

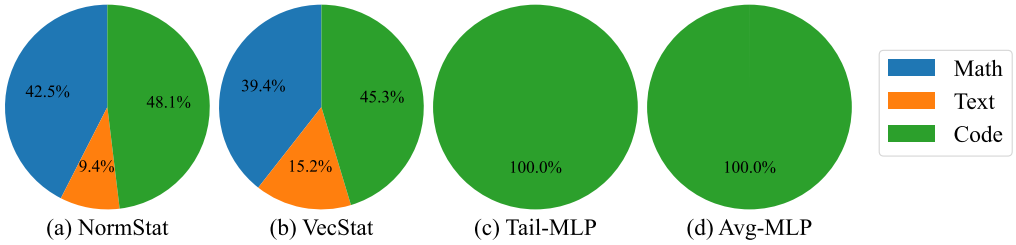


Figure 7: Uncertainty quantification results on mixed-intent prompt with reversed concatenation order (mathematical contents followed by code contents) on Qwen3-1.7B-Base.

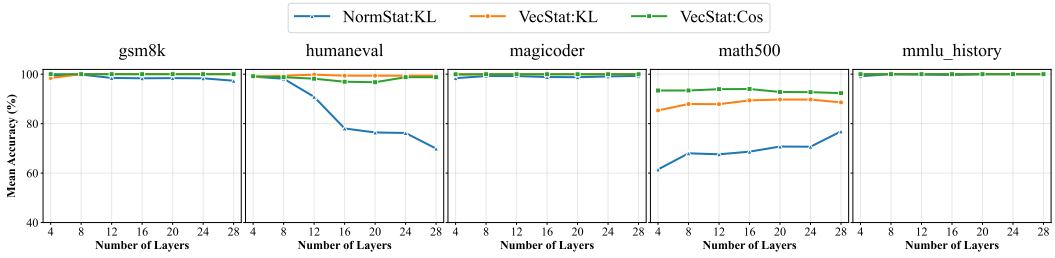


Figure 8: Effect of the number of layers on level-1 classification accuracy for Qwen3-1.7B.
```

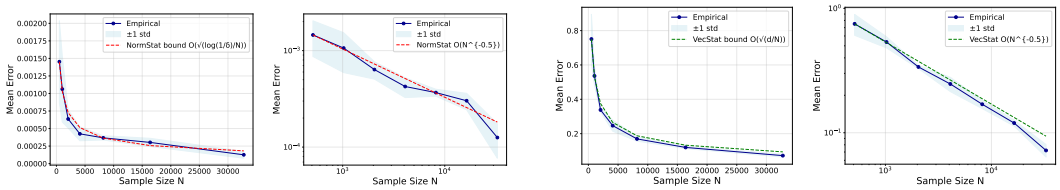

(a) Llama-3.2-1B-Instruct (NormStat)

(b) Llama-3.2-1B-Instruct (VecStat)

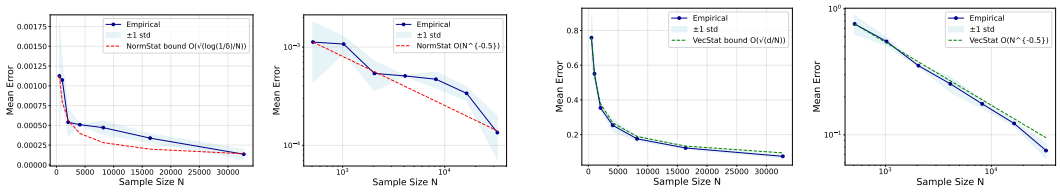

(c) Llama-3.2-1B (NormStat)

(d) Llama-3.2-1B (VecStat)

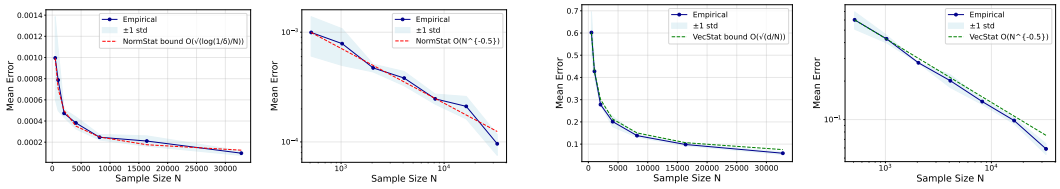

(e) Qwen3-1.7B-Base (NormStat)

(f) Qwen3-1.7B-Base (VecStat)

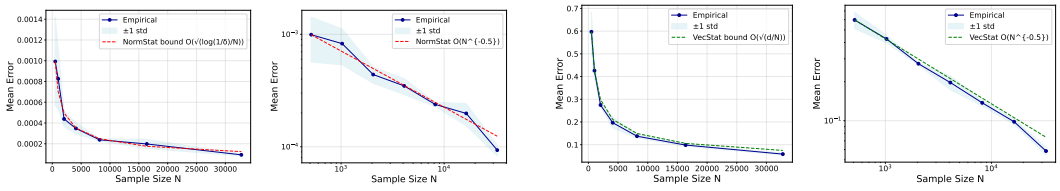

(g) Qwen3-1.7B (NormStat)

(h) Qwen3-1.7B (VecStat)

Figure 9: Calibration convergence analysis for different models and methods on the MagiCoder dataset. Each subplot shows both linear and log-log scales comparing empirical results with theoretical bounds. NormStat (norm method) uses dimension-free bounds while VecStat (projection method) uses dimension-dependent bounds.

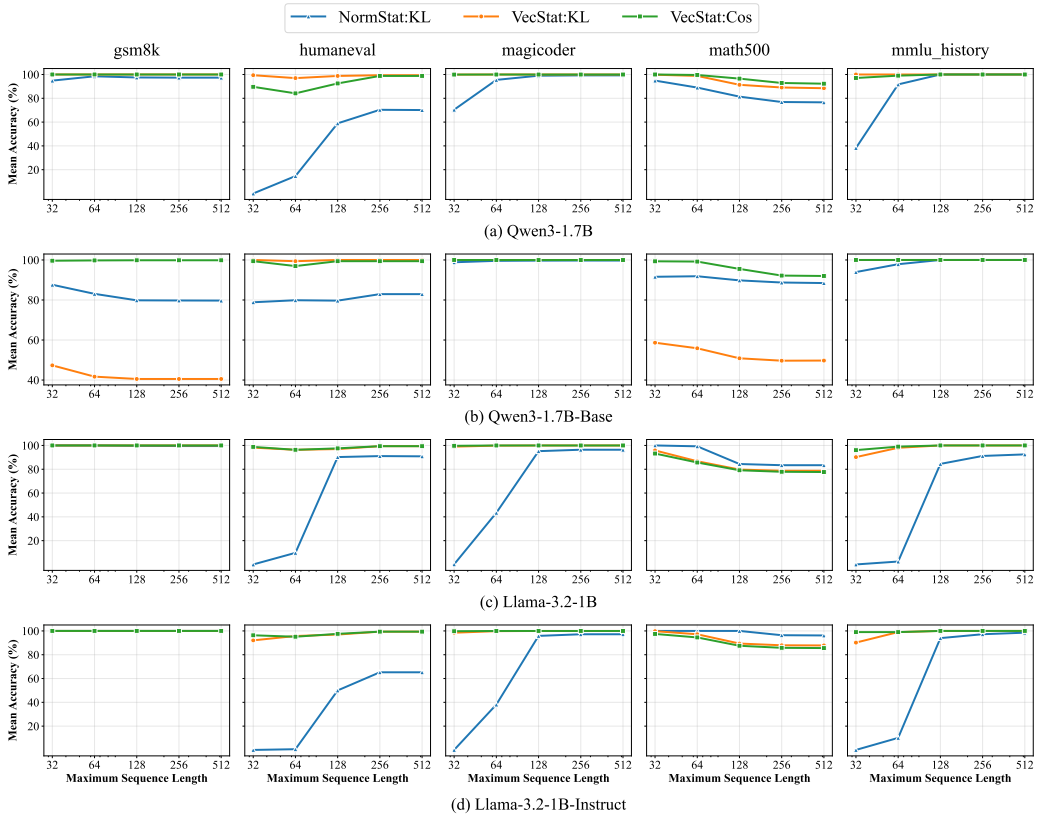

Figure 10: Effect of the maximum prompt length on level-1 classification accuracy for Qwen3-1.7B (a), Qwen3-1.7B-Base (b), Llama-3.2-1B (c), and Llama-3.2-1B-Instruct (d)..